

Bayesian Regression Using a Prior on the Model Fit: The R²-D² Shrinkage Prior

Yan Dora Zhang¹, Brian P. Naughton², Howard D. Bondell³, and Brian J. Reich²

¹*Department of Statistics and Actuarial Science, The University of Hong Kong*

²*Department of Statistics, North Carolina State University*

³*School of Mathematics and Statistics, University of Melbourne*

July 9, 2020

Abstract

Prior distributions for high-dimensional linear regression require specifying a joint distribution for the unobserved regression coefficients, which is inherently difficult. We instead propose a new class of shrinkage priors for linear regression via specifying a prior first on the model fit, in particular, the coefficient of determination, and then distributing through to the coefficients in a novel way. The proposed method compares favorably to previous approaches in terms of both concentration around the origin and tail behavior, which leads to improved performance both in posterior contraction and in empirical performance. The limiting behavior of the proposed prior is $1/x$, both around the origin and in the tails. This behavior is optimal in the sense that it simultaneously lies on the boundary of being an improper prior both in the tails and around the origin. None of the existing shrinkage priors obtain this behavior in both regions simultaneously. We also demonstrate that our proposed prior leads to the same near-minimax posterior contraction rate as the spike-and-slab prior.

Keywords: Global-Local Shrinkage, High-dimensional regression, Beta-prime distribution, Coefficient of Determination

1 Introduction

Consider the linear regression model,

$$Y_i = \mathbf{x}_i^T \boldsymbol{\beta} + \varepsilon_i, \quad i = 1, \dots, n, \quad (1)$$

where Y_i is the i th response, \mathbf{x}_i is the p -dimensional vector of covariates for the i th observation, $\boldsymbol{\beta} = (\beta_1, \dots, \beta_p)^T$ is the coefficient vector, and the ε_i 's are the error terms assumed to be normal and independent with $E(\varepsilon_i) = 0$ and $\text{var}(\varepsilon_i) = \sigma^2$. High-dimensional data with $p > n$ in this context is common in diverse application areas. It is well known that maximum likelihood estimation performs poorly in this setting, and this motivates a number of approaches in shrinkage estimation and variable selection. In the Bayesian framework, there are two main approaches to address such problems: two component discrete mixture prior (also referred as spike and slab prior) and continuous shrinkage priors. The discrete mixture priors (George & McCulloch 1993, Ishwaran & Rao 2005, Mitchell & Beauchamp 1988, Narisetty & He 2014) put a point mass (spike) at $\beta_j = 0$ and a continuous prior (slab) for the terms with $\beta_j \neq 0$. Although these priors have an intuitive and appealing representation, they lead to computational issues due to the spread of posterior probability over the 2^p models formed by including subsets of the coefficients to zero. Implementation instead can proceed by applying approximation methods, such as stochastic search variable selection (George & McCulloch 1993), shotgun stochastic search (Hans et al. 2007), variational Bayes (Ormerod et al. 2017), and EM (Ročková & George 2014) all of which have improved the computational feasibility and include theoretical underpinnings.

The computation issues with discrete mixture priors motivate continuous shrinkage priors. The shrinkage priors are essentially written as global-local scale mixture Gaussian family as summarized in Polson & Scott (2010), i.e.,

$$\beta_j \mid \phi_j, \omega \sim N(0, \omega \phi_j), \quad \phi_j \sim \pi(\phi_j), \quad (\omega, \sigma^2) \sim \pi(\omega, \sigma^2),$$

where ω represents the global shrinkage, while ϕ_j 's are the local variance components. Current existing global-local priors exhibit desirable theoretic and empirical properties. They can shrink the overall signal, while varying the amount of shrinkage on different components. These continuous priors exhibit both heavy tails and high concentration around

zero. The heavy tail reduces the bias in estimation of large coefficients, while the high concentration around zero shrinks the irrelevant coefficients heavily to zero, thus reducing the noise. Some examples include Normal-Gamma mixtures (Griffin & Brown 2010), Horseshoe (Carvalho et al. 2009, 2010), generalized Beta (Armagan et al. 2011), generalized double Pareto (Armagan, Dunson & Lee 2013), Dirichlet-Laplace (Bhattacharya et al. 2015), Horseshoe+ (Bhadra et al. 2016), normal-beta prime prior (Bai & Ghosh 2019).

In general, it is difficult to specify a p -dimensional prior on β , particularly with high dimensional data. Instead, we propose to first construct a prior on the coefficient of determination, R^2 , for which the model-based version is defined as the square of the correlation coefficient between the dependent variable and its modeled expectation. A prior on this one-number summary forms a prior on a function of the parameter vector, and is then distributed through to the individual parameters in a natural way. We develop a class of priors that are constructed via marginalizing over the design, as well as those conditioning on the design. By viewing things in this framework, our proposed class of priors are induced by a Beta(a, b) prior on R^2 and lead to priors having desirable properties both asymptotically and in finite samples.

We show that our class of priors, which we term the R^2 -induced Dirichlet Decomposition (R2-D2) priors, simultaneously obtain both heavier tails and tighter concentration around zero than all previously proposed approaches. This optimal result translates into improved performance in estimation and inference. We also offer a theoretical framework to compare different global-local priors. The proposed method compares favorably to the other global-local shrinkage priors in terms of both its concentration around the origin and its tail behavior obtaining a limiting behavior of $1/x$ in both regions. This behavior is optimal in the sense that it simultaneously lies on the boundary of being an improper prior in both areas, and translates into improved theoretical and empirical performance.

The rest of the paper is outlined as follows. Section 2 motivates the idea of inducing a prior via R^2 , and distinguishes between a marginal and conditional version. Section 3 presents the details of the conditional version in both the low- and high-dimensional settings. Section 4 details the marginal version and provides theoretical properties of both

the prior and the posterior. Section 5 discusses novel MCMC algorithms for computation of both the conditional and marginal versions, while Section 6 provides simulation results. Section 7 provides real data examples. All proofs are given in the Appendix.

2 Motivation

The typical Bayesian approach specifies a joint distribution on the model parameters, namely for the regression coefficients and error variance. Instead, we specify a distribution for R^2 with practical meaning, and then induce a prior on the p -dimensional $\boldsymbol{\beta}$.

Suppose that the predictor vector for each observation $\mathbf{x} \sim H(\cdot)$, with $E(\mathbf{x}) = \boldsymbol{\mu}$ and $\text{cov}(\mathbf{x}) = \Sigma$. Assume that \mathbf{x} is independent of the error, ε , and then the marginal variance of $y = \mathbf{x}^T \boldsymbol{\beta} + \varepsilon$ is $\text{var}(\mathbf{x}^T \boldsymbol{\beta}) + \sigma^2$. For simplicity, we assume that the response is centered and covariates are standardized so that $\boldsymbol{\mu} = \mathbf{0}$, there is no intercept term in (1), and all diagonal elements of Σ are 1. The coefficient of determination, R^2 , can be calculated as the square of the correlation coefficient between the dependent variable, y , and the modeled value, $\mathbf{x}^T \boldsymbol{\beta}$, i.e.,

$$R^2 = \frac{\text{cov}^2(y, \mathbf{x}^T \boldsymbol{\beta})}{\text{var}(y)\text{var}(\mathbf{x}^T \boldsymbol{\beta})} = \frac{\text{cov}^2(\mathbf{x}^T \boldsymbol{\beta} + \varepsilon, \mathbf{x}^T \boldsymbol{\beta})}{\text{var}(\mathbf{x}^T \boldsymbol{\beta} + \varepsilon)\text{var}(\mathbf{x}^T \boldsymbol{\beta})} = \frac{\text{var}(\mathbf{x}^T \boldsymbol{\beta})}{\text{var}(\mathbf{x}^T \boldsymbol{\beta}) + \sigma^2}. \quad (2)$$

A hypothesized value of R^2 has been used previously to tune informative priors, and to select hyper-parameters for regularization problems. Scott & Varian (2014) elicit an informative distribution for the error variance, σ^2 , based on elicitation of the expected R^2 , and the response. Zhang & Bondell (2018) proposed to choose hyper-parameters for shrinkage priors by empirically minimizing the Kullback-Leibler divergence between the expected distribution of R^2 and a Beta distribution. Here, in contrast, we develop our approach from first principles via placing a prior distribution on R^2 directly, rather than using a hypothesized value as a tool to tune parameters in already existing priors.

Based on this representation of R^2 , two alternative approaches can be taken to construction of the prior. A conditional version places a Beta prior on the conditional distribution of R^2 which depends on the model design, \mathbf{X} . Conversely, a marginal version assumes that the marginal distribution of R^2 (after integrating out $\boldsymbol{\beta}$ and \mathbf{X}) has a Beta distribution.

The former has the interpretation of the usual sample-based version of R^2 , while the latter allows for more direct asymptotic analysis of the posterior, as the design is integrated out. We will show that both versions lead to priors having different, but desirable properties.

3 Conditional R^2 Prior

3.1 R^2 as Elliptical Contours

We now introduce the conditional version, which, conditioning on the design points, yields

$$R^2(\boldsymbol{\beta}) = \frac{\boldsymbol{\beta}^T \mathbf{X}^T \mathbf{X} \boldsymbol{\beta}}{\boldsymbol{\beta}^T \mathbf{X}^T \mathbf{X} \boldsymbol{\beta} + n\sigma^2}. \quad (3)$$

We specifically write $R^2(\boldsymbol{\beta})$ to reflect the fact that R^2 depends on the unknown vector $\boldsymbol{\beta}$ (as well as σ^2). Notice that (3) will reduce to the familiar sample statistic, R^2 , if the least-squares estimates were substituted for $\boldsymbol{\beta}$ and σ^2 . Conditional on σ^2 and \mathbf{X} , a distribution on R^2 induces a distribution on the quadratic form, $\boldsymbol{\beta}^T \mathbf{X}^T \mathbf{X} \boldsymbol{\beta}$.

We choose a Beta(a, b) prior for R^2 , where the choices of shape parameters a and b will determine the posterior behavior and will be discussed in more detail in the theoretical results and the implementation. An Inverse-Gamma(a_1, b_1) prior is used for σ^2 , but we note that other choices may also be applied. A prior for $\boldsymbol{\beta}$ given (R^2, σ^2) then must be defined on the surface of the ellipsoid: $\{\boldsymbol{\beta} : \boldsymbol{\beta}^T \mathbf{X}^T \mathbf{X} \boldsymbol{\beta} = nR^2\sigma^2/(1 - R^2)\}$. When $\mathbf{X}^T \mathbf{X}$ is full rank we may choose $\boldsymbol{\beta}$ to be uniformly distributed on this ellipsoid; that is, the distribution of $\boldsymbol{\beta}$ is constant given the quadratic form. We call this choice the “uniform-on-ellipsoid” prior for $\boldsymbol{\beta}$, and show a connection to a variation on a mixture of g -priors. The following proposition shows that $\boldsymbol{\beta}$ given σ^2 has an elliptical distribution after integrating out R^2 .

Proposition 1. *If $R^2 \mid \sigma^2$ has a Beta(a, b) distribution and $\boldsymbol{\beta} \mid R^2$ has a uniform prior on the ellipsoid, then $\boldsymbol{\beta} \mid \sigma^2$ has the probability density function:*

$$p(\boldsymbol{\beta} \mid \sigma^2) = \frac{\Gamma(p/2) |\boldsymbol{\Sigma}_{\mathbf{X}}|^{1/2}}{B(a, b) \pi^{p/2}} (\sigma^2)^{-a} (\boldsymbol{\beta}^T \boldsymbol{\Sigma}_{\mathbf{X}} \boldsymbol{\beta})^{a-p/2} (1 + \boldsymbol{\beta}^T \boldsymbol{\Sigma}_{\mathbf{X}} \boldsymbol{\beta} / \sigma^2)^{-(a+b)}, \quad (4)$$

where $\boldsymbol{\beta} \in \mathbb{R}^p$, $\boldsymbol{\Sigma}_{\mathbf{X}} = \mathbf{X}^T \mathbf{X} / n$, and $B(\cdot, \cdot)$ denotes the Beta function.

As a special case, if $a = p/2$ and $b = 1/2$, then $\boldsymbol{\beta}$ has a multivariate Cauchy distribution with spread parameter $\boldsymbol{\Sigma}_{\mathbf{X}}/\sigma^2$. Zellner & Siow (1980) recommended these Cauchy priors for model selection problems. The next proposition shows that for $a \leq p/2$, the distribution in (4) is equivalent to a mixture of normals g -prior, with a hyperprior on g that is the product of Beta and Inverse-Gamma distributions.

Proposition 2. *If $\boldsymbol{\beta} \mid \sigma^2, z, w \sim N_p(\mathbf{0}, zw\sigma^2(\mathbf{X}^T \mathbf{X})^{-1})$, $z \sim \text{Inverse-Gamma}(b, n/2)$, $w \sim \text{Beta}(a, p/2 - a)$, and $a \leq p/2$, then $\boldsymbol{\beta} \mid \sigma^2$ has the distribution given by the density in (4).*

This representation eases the posterior computations for a Gibbs sampler discussed in Section 5.

3.2 Sparse Regression and Local Shrinkage

The prior on R^2 regulates $\boldsymbol{\beta}$ through the quadratic form $\boldsymbol{\beta}^T \boldsymbol{\Sigma}_{\mathbf{X}} \boldsymbol{\beta}$, which can shrink the regression coefficients globally, but lacks the flexibility to handle different forms of sparsity. In addition, the posterior is not a proper distribution when \mathbf{X} is not full rank (e.g. when $n < p$). Rather than letting $\boldsymbol{\beta} \mid (R^2, \sigma^2)$ be uniformly distributed on the ellipsoid, we put a Normal-Gamma prior on $\boldsymbol{\beta}$ (Griffin & Brown 2010), but restrict its support to lie on the surface of the ellipsoid. Specifically, we let

$$\boldsymbol{\beta} \mid (R^2, \sigma^2, \boldsymbol{\Lambda}) \sim N_p\left(\mathbf{0}, \frac{\sigma^2 R^2}{1 - R^2} \boldsymbol{\Lambda}\right) \mathbb{1}\left\{\boldsymbol{\beta}^T \boldsymbol{\Sigma}_{\mathbf{X}} \boldsymbol{\beta} = \frac{\sigma^2 R^2}{1 - R^2}\right\} \quad (5)$$

$$\lambda_j \sim \text{Gamma}(\nu, \mu), \text{ for } j = 1, \dots, p, \quad (6)$$

where $\text{Gamma}(\nu, \mu)$ represents Gamma distribution with shape parameter ν and rate parameter μ , $\boldsymbol{\Lambda} = \text{diag}\{\lambda_1, \dots, \lambda_p\}$ and $\mathbb{1}\{\cdot\}$ is the indicator function. Note that this prior no longer requires $\boldsymbol{\Sigma}_{\mathbf{X}}$ to be full rank for it to be proper. Proposition 3 shows that the induced model described in the previous section is a special case of the hierarchical model proposed here with fixed $\boldsymbol{\Lambda}$.

Proposition 3. *If $\boldsymbol{\beta} \mid (R^2, \sigma^2, \boldsymbol{\Lambda})$ has the distribution in (5), and $\boldsymbol{\Lambda} = (\mathbf{X}^T \mathbf{X})^{-1}$, then $\boldsymbol{\beta} \mid \sigma^2$ has the distribution in (4).*

That is, if the contours of the Normal distribution align with the ellipsoid, then we recover the uniform-on-ellipsoid prior.

In general, the conditional distribution of $\boldsymbol{\beta}$ is similar to a Bingham distribution, which is a multivariate Normal distribution conditioned to lie on the unit sphere. This Bingham distribution has density $f(\boldsymbol{w} \mid \mathbf{A}) = C_A^{-1} \exp\{-\boldsymbol{w}^T \mathbf{A} \boldsymbol{w}\}$ with respect to the uniform measure on the $p - 1$ dimensional unit sphere, where C_A is the normalizing constant (Bingham 1974). Here, $\boldsymbol{\beta} \mid (R^2, \sigma^2, \mathbf{A})$ is a Bingham distributed random vector that has been rotated and scaled to lie on the ellipsoid rather than the unit sphere. The matrix \mathbf{X} determines the rotation of the ellipsoid, R^2 and σ^2 determine the size of the ellipsoid, and the conditional prior on $\boldsymbol{\beta}$ determines the direction to the surface. If the local variance components (λ_j) are small, then regions of the ellipsoid near the axes will be favored, encouraging sparser estimates. Like the Normal-Gamma priors, this is primarily controlled by the shape parameter, ν . Figure 1 illustrates the local shrinkage properties of the prior, showing 10,000 samples of $\boldsymbol{\beta} \mid (R^2, \sigma^2)$. Default choices of the hyper-parameters ν and μ follow from the recommendations of Griffin & Brown (2010) and are discussed in the implementation in Section 6.

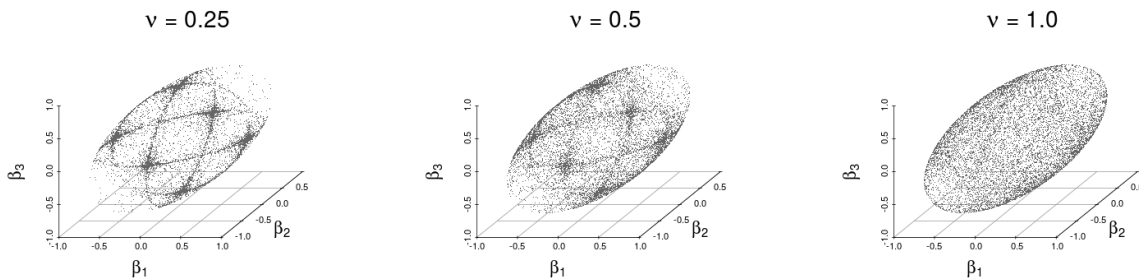


Figure 1: 10,000 samples from the prior of $\boldsymbol{\beta} \mid (R^2, \sigma^2)$ for different choices of ν .

4 Marginal R^2 Prior

4.1 The R2-D2 Global-Local Shrinkage Prior

Rather than conditioning on the design \mathbf{X} , we now instead show how to construct a prior while marginalizing out both $\boldsymbol{\beta}$ and the design. While the conditional version retains the interpretation of R^2 as elliptical contours in the design space, the marginal version allows for an in depth study of the asymptotic properties of both the prior and the resulting posterior.

Consider a prior for $\boldsymbol{\beta}$ satisfying $E(\boldsymbol{\beta}) = \mathbf{0}$ and $\text{cov}(\boldsymbol{\beta}) = \sigma^2 \boldsymbol{\Lambda}$, where $\boldsymbol{\Lambda}$ is a diagonal matrix with diagonal elements $\lambda_1, \dots, \lambda_p$. Then

$$\begin{aligned} \text{var}(\mathbf{x}^T \boldsymbol{\beta}) &= E_{\mathbf{x}}\{\text{var}_{\boldsymbol{\beta}}(\mathbf{x}^T \boldsymbol{\beta} \mid \mathbf{x})\} + \text{var}_{\mathbf{x}}\{E_{\boldsymbol{\beta}}(\mathbf{x}^T \boldsymbol{\beta} \mid \mathbf{x})\} = E_{\mathbf{x}}(\sigma^2 \mathbf{x}^T \boldsymbol{\Lambda} \mathbf{x}) + \text{var}_{\mathbf{x}}(0) \\ &= \sigma^2 E_{\mathbf{x}}\{\text{tr}(\mathbf{x}^T \boldsymbol{\Lambda} \mathbf{x})\} = \sigma^2 \text{tr}\{\boldsymbol{\Lambda} E_{\mathbf{x}}(\mathbf{x} \mathbf{x}^T)\} = \sigma^2 \text{tr}(\boldsymbol{\Lambda} \boldsymbol{\Sigma}) = \sigma^2 \sum_{j=1}^p \lambda_j. \end{aligned}$$

Then R^2 is represented as

$$R^2 = \frac{\text{var}(\mathbf{x}^T \boldsymbol{\beta})}{\text{var}(\mathbf{x}^T \boldsymbol{\beta}) + \sigma^2} = \frac{\sigma^2 \sum_{j=1}^p \lambda_j}{\sigma^2 \sum_{j=1}^p \lambda_j + \sigma^2} = \frac{\sum_{j=1}^p \lambda_j}{\sum_{j=1}^p \lambda_j + 1} \equiv \frac{W}{W + 1}, \quad (7)$$

where $W \equiv \sum_{j=1}^p \lambda_j$ is the sum of the prior variances scaled by σ^2 .

Similarly as conditional R^2 prior, we also assume $R^2 \sim \text{Beta}(a, b)$, a Beta distribution with shape parameters a and b . Then in this case, the induced prior density for $W = R^2/(1 - R^2)$ is a Beta Prime distribution (Johnson et al. 1995) denoted as $\text{BP}(a, b)$, with probability density function

$$\pi_W(x) = \frac{\Gamma(a + b)}{\Gamma(a)\Gamma(b)} \frac{x^{a-1}}{(1 + x)^{a+b}}, \quad (x > 0).$$

Therefore $W \sim \text{BP}(a, b)$ is equivalent to $R^2 \sim \text{Beta}(a, b)$. The following section will induce a prior on $\boldsymbol{\beta}$ based on the distribution of the sum of prior variances, W .

Any prior of the form $E(\boldsymbol{\beta}) = \mathbf{0}$, $\text{cov}(\boldsymbol{\beta}) = \sigma^2 \boldsymbol{\Lambda}$ and $W = \sum_{j=1}^p \lambda_j \sim \text{BP}(a, b)$ induces a $\text{Beta}(a, b)$ prior on R^2 . To construct a prior with such properties, we follow the global-local

prior framework and express $\lambda_j = \phi_j \omega$ with $\sum_{j=1}^p \phi_j = 1$. Then $W = \sum_{j=1}^p \phi_j \omega = \omega$ is the total prior variability, and ϕ_j is the proportion of total variance allocated to the j -th covariate. It is natural to assume that $\omega \sim \text{BP}(a, b)$ and the variances across covariates have a Dirichlet prior with concentration parameter (a_π, \dots, a_π) , i.e., $\phi = (\phi_1, \dots, \phi_p) \sim \text{Dir}(a_\pi, \dots, a_\pi)$. Since $\sum_{j=1}^p \phi_j = 1$, $\text{E}(\phi_j) = 1/p$, and $\text{var}(\phi_j) = (p-1)/\{p^2(pa_\pi+1)\}$, then smaller a_π would lead to larger variance of ϕ_j , $j = 1, \dots, p$, thus more ϕ_j would be close to zero with only a small proportion of larger components; while larger a_π would lead to smaller variance of ϕ_j , $j = 1, \dots, p$, thus producing a more uniform ϕ , i.e., $\phi \approx (1/p, \dots, 1/p)$. So a_π controls the sparsity of the model.

To fully define the global-local prior, we further need to assign a kernel distribution on each dimension of β . Since the Laplace distribution ensures more mass around zero and heavier tails than the normal kernel, we consider a Laplace prior on β_j for $j = 1, \dots, p$. The prior is then summarized as

$$\beta_j \mid \sigma^2, \phi_j, \omega \sim \text{DE}(\sigma(\phi_j \omega / 2)^{1/2}), \quad \phi \sim \text{Dir}(a_\pi, \dots, a_\pi), \quad \omega \sim \text{BP}(a, b), \quad (8)$$

where $\text{DE}(\delta)$ denotes a double-exponential distribution (i.e., Laplace distribution) with mean 0 and variance $2\delta^2$. Such prior is induced by a prior on R^2 and the total prior variance of β is decomposed through a Dirichlet prior, therefore we refer to the prior as the R^2 -induced Dirichlet Decomposition (R2-D2) prior. Here ω controls the global shrinkage degree through a and b , while ϕ_j controls the local shrinkage through a_π . Assume the variance $\sigma^2 \sim \text{Inverse-Gamma}(a_1, b_1)$, an inverse Gamma distribution with shape and scale parameters a_1 and b_1 respectively.

Proposition 4. *If $\omega \mid \xi \sim \text{Ga}(a, \xi)$ and $\xi \sim \text{Ga}(b, 1)$, then $\omega \sim \text{BP}(a, b)$, where $\text{Ga}(\mu, \nu)$ is the Gamma random variable with shape μ and rate ν .*

By applying above Proposition 4, the prior in (8) can also be written as

$$\beta_j \mid \sigma^2, \phi_j, \omega \sim \text{DE}(\sigma(\phi_j \omega / 2)^{1/2}), \quad \phi \sim \text{Dir}(a_\pi, \dots, a_\pi), \quad \omega \mid \xi \sim \text{Ga}(a, \xi), \quad \xi \sim \text{Ga}(b, 1).$$

Proposition 5. *If $\omega \mid \xi \sim \text{Ga}(a, \xi)$, $(\phi_1, \dots, \phi_p) \sim \text{Dir}(a_\pi, \dots, a_\pi)$, and $a = pa_\pi$, then it follows $\phi_j \omega \mid \xi \sim \text{Ga}(a_\pi, \xi)$, $j = 1, \dots, p$ independently.*

Thus, by Proposition 5, when $a = pa_\pi$, prior in (8) can also be written as

$$\beta_j \mid \sigma^2, \lambda_j \sim \text{DE}(\sigma(\lambda_j/2)^{1/2}), \lambda_j \sim \text{BP}(a_\pi, b). \quad (9)$$

or equivalently

$$\beta_j \mid \sigma^2, \lambda_j \sim \text{DE}(\sigma(\lambda_j/2)^{1/2}), \lambda_j \mid \xi \sim \text{Ga}(a_\pi, \xi), \xi \sim \text{Ga}(b, 1). \quad (10)$$

We set $a = pa_\pi$ in the rest of the paper for the R2-D2 prior.

4.2 Properties of the R2-D2 Prior

In this section, the marginal density as well as its theoretical properties of the proposed R2-D2 prior are established. The properties of the Horseshoe (Carvalho et al. 2009, 2010), Horseshoe+ (Bhadra et al. 2016), generalized double Pareto prior (Armagan, Dunson & Lee 2013) and Dirichlet-Laplace prior (Bhattacharya et al. 2015) are provided as a comparison. Proofs and technical details are given in the Appendix.

For simplicity of comparison across different priors, the variance term σ^2 is fixed at 1.

Proposition 6. *Given the R2-D2 prior (9), the marginal density of β_j for any $j = 1, \dots, p$ is*

$$\pi_{R2-D2}(\beta_j) = \frac{G_{1,3}^{3,1} \left(\frac{\beta_j^2}{2} \mid \frac{1}{2}-b, a_\pi-\frac{1}{2}, 0, \frac{1}{2} \right)}{(2\pi)^{1/2}\Gamma(a_\pi)\Gamma(b)} = \frac{G_{3,1}^{1,3} \left(\frac{2}{\beta_j^2} \mid \frac{3}{2}-a_\pi, 1, \frac{1}{2} \right)}{(2\pi)^{1/2}\Gamma(a_\pi)\Gamma(b)}$$

where $\Gamma(\cdot)$ denotes the Gamma function and $G_{p,q}^{m,n} \left(z \mid \begin{smallmatrix} b_1, \dots, b_q \\ a_1, \dots, a_p \end{smallmatrix} \right)$ denotes the Meijer G-function (see Appendix for the detailed definition).

Now we would like to compare the theoretical properties with our proposed R2-D2 prior with a couple of common global-local shrinkage priors. We first listed these priors.

The Horseshoe prior proposed in Carvalho et al. (2009, 2010) is

$$\beta_j \mid \lambda_j \sim N(0, \lambda_j^2), \lambda_j \mid \tau \sim C^+(0, \tau),$$

where $C^+(0, \tau)$ denotes a half-Cauchy distribution with scale parameter τ , with density $\pi(y \mid \tau) = 2/\{\pi\tau(1 + (y/\tau)^2)\}$.

The Horseshoe+ prior proposed in Bhadra et al. (2016) is

$$\beta_j \mid \lambda_j \sim N(0, \lambda_j^2), \lambda_j \mid \tau, \eta_j \sim C^+(0, \tau \eta_j), \eta_j \sim C^+(0, 1).$$

The Dirichlet-Laplace prior proposed in Bhattacharya et al. (2015) is

$$\beta_j \mid \psi_j \sim \text{DE}(\psi_j), \psi_j \sim \text{Ga}(a^*, 1/2). \quad (11)$$

The normal-beta prime prior proposed in Bai & Ghosh (2019) is as follows:

$$\beta_j \mid \tau_j \sim N(0, \tau_j), \tau_j \sim \text{BP}(a^\#, b^\#). \quad (12)$$

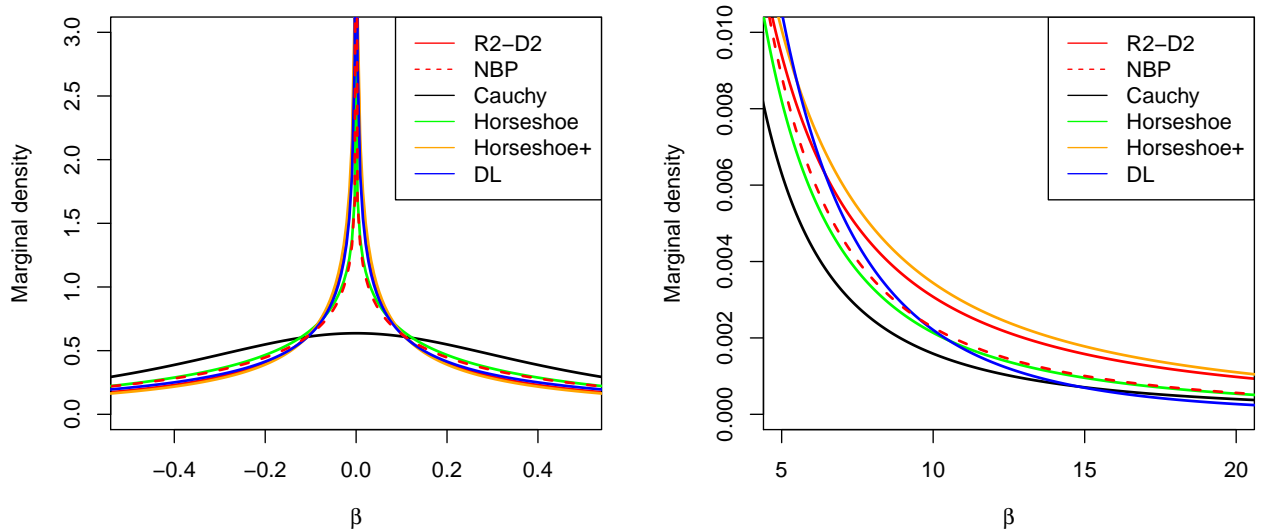


Figure 2: Marginal density of the R2-D2 (R2-D2), normal-beta prime (NBP), Dirichlet-Laplace (DL), Horseshoe, Horseshoe+ prior and Cauchy distribution. In all cases, the hyper-parameters are selected to ensure the interquartile range is 1 for visual comparison.

Figure 2 plots the marginal density function of the R2-D2 density along with the normal-beta prime, Horseshoe, Horseshoe+, Dirichlet-Laplace, and Cauchy distributions. In the figure, for visual comparison, the hyper-parameter in the priors, i.e., τ in Horseshoe and Horseshoe+ prior, a^* in Dirichlet-Laplace prior, (a_π, b) in the R2-D2 prior, are selected to ensure the interquartile range is 1. Note that to make the plots comparable, a_π in the

proposed R2-D2 prior is set as $a^*/2$, which is half of the hyper-parameter in the Dirichlet-Laplace prior. It will be shown later that this results in the same behavior around the origin for the two priors. The other hyper-parameter b in the R2-D2 prior is then tuned to ensure the interquartile range of 1 to match the others. For the normal-beta prime prior, we follow the values in Bai & Ghosh (2019), i.e., $a^\# = 0.48$ and $b^\# = 0.52$ which also ensures an interquartile range of 1.

From the plot, it appears that the R2-D2 prior can obtain both the highest concentration around zero and heaviest tail simultaneously. We will quantify these rates exactly in the next subsection, in Table 1. In particular, we will see that the R2-D2 prior is the only one obtaining polynomial behavior in both regions.

In the normal means model, van der Pas et al. (2014) and van der Pas et al. (2017a) investigate the Horseshoe posterior contraction rate, Bhattacharya et al. (2015) shows the optimal posterior concentration results for Dirichlet-Laplace prior, Bhadra et al. (2016) proves that the Horseshoe+ posterior concentrates at a faster rate than Horseshoe in the Kullback-Leibler sense, and Bai & Ghosh (2019) shows that normal-beta prime prior leads to a near minimax posterior concentration rate.

In this paper, we examine the concentration around zero and tail behaviors of the marginal densities of a number of priors, and show that our proposed approach simultaneously achieves high concentration at the origin and heavy tails. We will also study the posterior consistency and contraction properties in the high-dimensional regression model setup. As shown in Figure 2, all five global-local shrinkage priors have a marginal density with a singularity at zero while with different concentration rate. Except for the Dirichlet-Laplace prior, all other priors' marginal density have a heavier tail than the Cauchy distribution. We formally investigate their marginal densities' properties in the following sections.

4.2.1 Asymptotic tail behaviors

We examine the behavior of the tails of the proposed R2-D2 prior in this section. A prior with heavy tails is desirable in high-dimensional regression to allow the posterior to estimate

large values for important predictors.

Theorem 1. *Given $|\beta| \rightarrow \infty$, for any $a_\pi > 0$ and $b > 0$, the marginal density of the R2-D2 prior (9) satisfies $\pi_{R2-D2}(\beta) = O(1/|\beta|^{2b+1})$. Furthermore, when $0 < b < 1/2$, $\lim_{|\beta| \rightarrow \infty} \pi_{R2-D2}(\beta)/\beta^{-2} = \infty$, i.e., the R2-D2 prior has heavier tails than the Cauchy distribution.*

With a polynomial tail heavier than Cauchy distribution, the proposed R2-D2 prior attains a substantial improvement over a large class of global-local shrinkage priors.

As a comparison, we study the tail behavior of the Dirichlet-Laplace and double Pareto prior. The density of generalized double Pareto prior proposed in Armagan, Dunson & Lee (2013) is

$$\pi_{GDP}(\beta_j | \eta, \alpha) = (1 + |\beta_j|/\eta)^{-(\alpha+1)}/(2\eta/\alpha), \quad (\alpha, \eta > 0).$$

Theorem 2. *Given $|\beta| \rightarrow \infty$, for any $\alpha > 0$, the marginal density of the generalized double Pareto prior satisfies $\pi_{GDP}(\beta) = O(1/|\beta|^{\alpha+1})$. Furthermore, when $\alpha < 1$, $\lim_{|\beta| \rightarrow \infty} \pi_{GDP}(\beta)/\beta^{-2} = \infty$, i.e., the double Pareto prior has heavier tails than the Cauchy distribution.*

Theorem 3. *Given $|\beta| \rightarrow \infty$, for any $a^* > 0$, the marginal density of the Dirichlet-Laplace prior as shown in (11) satisfies $\pi_{DL}(\beta) = O(|\beta|^{a^*/2-3/4}/\exp\{\sqrt{2|\beta|}\})$. Furthermore, $\lim_{|\beta| \rightarrow \infty} \pi_{DL}(\beta)/\beta^{-2} = 0$, i.e., the Dirichlet-Laplace prior has lighter tails than the Cauchy distribution.*

As noted in Carvalho et al. (2010), the Horseshoe prior has exact Cauchy-like tails that decay like β^{-2} , and the Horseshoe+ prior has a tail of $O(\log(|\beta|)/\beta^2)$ as illustrated in the proof of Theorem 4.6 in Bhadra et al. (2016). Therefore, the double Pareto prior and the proposed R2-D2 prior lead to the heaviest tail, followed by Horseshoe+, then Horseshoe, and finally Dirichlet-Laplace prior.

4.2.2 Concentration properties

In this section, we study the concentration properties of the R2-D2 prior around the origin. The concentration properties of Dirichlet-Laplace, Horseshoe, and Horseshoe+ priors are

also given. We favor priors with high concentration near zero to reflect the prior that most of the covariates do not have a substantial effect on the response. We now show that R2-D2 prior has higher concentration at zero to go along with heavier tails than other global-local priors.

Theorem 4. *As $|\beta| \rightarrow 0$, if $0 < a_\pi < 1/2$ and $b > 0$, the marginal density of the R2-D2 prior as shown in (9) satisfies $\pi_{R2-D2}(\beta) = O(1/|\beta|^{1-2a_\pi})$.*

Theorem 5. *As $|\beta| \rightarrow 0$, if $0 < a^* < 1$, the marginal density of the Dirichlet-Laplace prior as shown in (11) satisfies $\pi_{DL}(\beta) = O(1/|\beta|^{1-a^*})$.*

For the Horseshoe prior, as summarized in Carvalho et al. (2010), the marginal density $\pi_{HS}(\beta) = (2\pi^3)^{-1/2} \exp(\beta^2/2) E_1(\beta^2/2)$, where $E_1(z) = \int_1^\infty e^{-tz}/t dt$ is the exponential integral function. As $|\beta| \rightarrow 0$,

$$\frac{1}{2(2\pi^3)^{1/2}} \log(1 + \frac{4}{\beta^2}) \leq \pi_{HS}(\beta) \leq \frac{1}{(2\pi^3)^{1/2}} \log(1 + \frac{2}{\beta^2}).$$

Therefore around the origin, $\pi_{HS}(\beta) = O(\log(1/|\beta|))$. Also by the proof of Theorem 4.6 in Bhadra et al. (2016), as $|\beta| \rightarrow 0$, the marginal density of Horseshoe+ prior satisfies $\pi_{HS+}(\beta) = O(\log^2(1/|\beta|))$.

It is clear that $2a_\pi$ in the R2-D2 prior plays the same role around the origin as a_D in the Dirichlet-Laplace prior. Accordingly, when $a^* = 2a_\pi \in (0, 1)$, all these four priors possess unbounded density near the origin. However, the R2-D2 prior and Dirichlet-Laplace prior diverge to infinity with a polynomial order, much faster than the Horseshoe+ (with a squared logarithm order) and the Horseshoe prior (with a logarithm order). Although the double Pareto prior also has a polynomial order tail similar as our proposed R2-D2 prior, the double Pareto prior differs around the origin, as it remains bounded, while our proposed R2-D2 prior is unbounded at the origin. As for the normal-beta prime prior, we show that its concentration rate is slower than the R2-D2 prior.

The results for all priors in both tail behavior and concentration around zero are summarized in Table 1. The proposed R2-D2 prior is the only one that can achieve polynomial rates both in the tails as well as around zero. This is the limiting case in that it can then be arbitrarily close to the boundary case of $1/|\beta|$ in each region.

	Tail Decay	Concentration at zero
Horseshoe	$O\left(\frac{1}{\beta^2}\right)$	$O\left(\log\left(\frac{1}{ \beta }\right)\right)$
Horseshoe+	$O\left(\frac{\log \beta }{\beta^2}\right)$	$O\left(\log^2\left(\frac{1}{ \beta }\right)\right)$
Dirichlet-Laplace	$O\left(\frac{ \beta ^{\alpha^*/2-3/4}}{\exp\{\sqrt{2} \beta \}}\right)$	$O\left(\frac{1}{ \beta ^{1-\alpha^*}}\right)$
Generalized Double Pareto	$O\left(\frac{1}{ \beta ^{1+\alpha}}\right)$	$O(1)$
R2-D2	$O\left(\frac{1}{ \beta ^{1+2b}}\right)$	$O\left(\frac{1}{ \beta ^{1-2a\pi}}\right)$

Table 1: Tail behavior and concentration around zero for Horseshoe, Horseshoe+, Dirichlet-Laplace, Generalized Double Pareto, and R2-D2 priors.

4.2.3 Consistency and contraction of R2-D2 Posterior

In what follows, we rewrite p as p_n to indicate the dimension of β_n can increase with the sample size n . We denote the true regression parameter as β_n^0 . Let q_n be the number of nonzero components in β_n^0 . We use $\|\cdot\|$ as the L_2 norm, and $\|\cdot\|_1$ as L_1 norm for vectors, respectively. Denote $\mathbf{Y}_n = (Y_1, \dots, Y_n)^T$. Denote $\mathbf{X}_n = (\mathbf{x}_1^T, \dots, \mathbf{x}_n^T)^T$. Let ξ_n denote a set of indices where $\xi_n \subset \{1, \dots, p_n\}$, and let \mathbf{X}_{ξ_n} denote the sub-matrix of \mathbf{X}_n that contains the columns with indices in ξ_n . Denote ξ_n^0 as the set containing the nonzero indices of β_n^0 . For two positive sequences a_n and b_n , $a_n \asymp b_n$ means $0 < \liminf a_n/b_n \leq \limsup a_n/b_n < \infty$; $a_n \prec b_n$ means $a_n = o(b_n)$; $a_n \succ b_n$ means $b_n = o(a_n)$; $a_n \preceq b_n$ means either $a_n \prec b_n$ or $a_n \asymp b_n$; and $a_n \succeq b_n$ means either $a_n \succ b_n$ or $a_n \asymp b_n$.

We now show that the proposed R2-D2 prior yields strong posterior consistency in the case that $p_n \prec n$, and further that it attains the optimal near-minimax contraction rate in general, including with $p_n \succeq n$, as given by Castillo et al. (2015), Song & Liang (2017) and Ročková & George (2018).

Theorem 6 shows strong posterior consistency under $p_n = o(n)$, and assumes the following regularity conditions:

(A1) $p_n \prec n$;

(A2) Let d_{p_n} and d_1 be the smallest and the largest singular values of $\mathbf{X}_n^T \mathbf{X}_n/n$ respectively.

Assume $0 < d_{\min} < \liminf_{n \rightarrow \infty} d_{p_n} \leq \limsup_{n \rightarrow \infty} d_1 < d_{\max} < \infty$, where d_{\min} and d_{\max} are fixed;

(A3) $\max_{j=1, \dots, p_n} \{|\beta_{nj}^0|\} \leq E_n$ for some nondecreasing sequence, E_n , with $\log(E_n) = O(\log n)$;

(A4) $q_n = o(n/\log n)$.

Theorem 6. *Under assumptions (A1)–(A4), for any $b > 0$, given the linear regression model (1) with known σ^2 , if $a_\pi = C/(p_n^{b/2} n^{rb/2} \log n)$ for finite $r > 0$ and $C > 0$, then the R2-D2 prior (9) yields a strongly consistent posterior, i.e., for any $\epsilon > 0$,*

$$Pr_{\beta_n^0} \{ \pi_n(\beta_n : \|\beta_n - \beta_n^0\| \geq \epsilon \mid \mathbf{Y}_n) \rightarrow 0 \} = 1 \text{ as } n \rightarrow \infty.$$

Theorem 6 shows the posterior strong consistency of the R2-D2 prior under $p_n \prec n$. Furthermore, in the high dimensional case, with $p_n \succeq n$, we place an inverse-Gamma prior on σ^2 , and denote σ^0 as the true parameter value which is unknown but fixed. Theorem 7 shows that the R2-D2 prior contracts at the near-minimax rate in this regime, under the following regularity conditions:

(B1) All the covariates are uniformly bounded. For simplicity, we assume they are all bounded by 1;

(B2) $p_n \succeq n$;

(B3) There exists some integer \bar{p}_n and fixed constant d_0 such that $\bar{p}_n \succ q_n$ and the smallest singular value of matrix $\mathbf{X}_{\xi_n}^T \mathbf{X}_{\xi_n}/n$ is no smaller than d_0 for any subset model of size $|\xi_n| \leq \bar{p}_n$;

(B4) $\max_{j=1, \dots, p_n} \{|\beta_{nj}^0/\sigma^0|\} \leq E_n$ for some nondecreasing sequence, E_n , with $\log(E_n) = O(\log p_n)$.

(B5) $q_n = o(n/\log p_n)$;

Theorem 7. *Assume that (B1)–(B5) hold. Denote $\epsilon_n = M\sqrt{q_n(\log p_n)/n}$ where $M > 0$ is sufficiently large, and let $k_n \asymp \sqrt{q_n(\log p_n)/n}/p_n$. Given the linear regression model (1),*

suppose that we place an inverse-Gamma prior on σ^2 and place the R2-D2 prior (9) on β . For any $b > 0$, if $a_\pi \leq \log(1 - p_n^{-1+u})/(2 \log k_n)$ where $u > 0$, then the following hold:

$$\begin{aligned} Pr_{\beta_n^0} \left\{ \pi_n(\beta_n : \|\beta_n - \beta_n^0\| \geq c_1 \sigma^0 \epsilon_n \mid \mathbf{Y}_n) \geq e^{-c_2 n \epsilon_n^2} \right\} &\leq e^{-c_3 n \epsilon_n^2}, \\ Pr_{\beta_n^0} \left\{ \pi_n(\beta_n : \|\beta_n - \beta_n^0\|_1 \geq c_1 \sigma^0 \sqrt{q_n} \epsilon_n \mid \mathbf{Y}_n) \geq e^{-c_2 n \epsilon_n^2} \right\} &\leq e^{-c_3 n \epsilon_n^2}, \\ Pr_{\beta_n^0} \left\{ \pi_n(\beta_n : \|\mathbf{X}_n \beta_n - \mathbf{X}_n \beta_n^0\| \geq c_1 \sigma^0 \sqrt{n} \epsilon_n \mid \mathbf{Y}_n) \geq e^{-c_2 n \epsilon_n^2} \right\} &\leq e^{-c_3 n \epsilon_n^2}, \end{aligned}$$

for some positive constants c_1 , c_2 , and c_3 .

According to Raskutti et al. (2011), the minimax L_2 rate is $O(\sqrt{q_n \log(p_n/q_n)/n})$. For the R2-D2 prior, the L_2 and L_1 contraction rates for the posterior of β_n are $O(\sqrt{q_n (\log p_n)/n})$ and $O(q_n \sqrt{(\log p_n)/n})$, respectively. So the contraction rates of R2-D2 prior are near-minimax. Note that these rates are the same as the rates achieved by spike-and-slab approaches as in Castillo et al. (2015), Song & Liang (2017) and Ročková & George (2018).

We note that Theorem 6 shows strong consistency in the $p_n \prec n$ regime, while Theorem 7 shows the contraction rate for $p_n \succeq n$. While, the result in Theorem 7 is stronger, including stronger conditions on the hyperparameters, we do conjecture that the near-minimax contraction rate will also hold in the case of $p_n \prec n$, with a condition on the hyperparameters that is weaker than that of Theorem 7. As also pointed out in Song & Liang (2017), in this case it is not necessary to require a strong prior concentration which is ensured by the conditions of Theorem 7, and one only need to impose conditions on the local shape of the prior around the true β^0 .

4.2.4 Choice of Hyperparameters

Based on these properties, we now discuss a default choice of hyperparameters that can be implemented in practice. We set $a_\pi = a/p$ throughout, which is not as a choice, but it is an important step in the definition of the prior. The reason for this very specific relationship is to ensure that the R2-D2 prior in (8) can be re-written as (9) and (10). The theoretical properties are derived based on (9) (or (10)), hence they assume this specific form of a_π , as any other choice would no longer yield the same theoretical results. In addition, it ensures

that the MCMC algorithm is fully Gibbs sampling. With any other choice of a_π , this would not be the case, and a Metropolis step would be needed in the algorithm.

Hence there are then two parameters to set, a and b . Based on the consistency results, we suggest to set a as a function of b based on the condition of Theorem 6. This leads to just one tuning parameter b . This determines the tail behavior and then all other parameters are fixed from that. For a fully default method, we set $b = 0.5$ to yield Cauchy-like tails, but other choices of tail behavior are possible if desired.

To determine a and a_π from a choice of b , note that the condition for consistency in Theorem 6 requires that $a_\pi = C/(p_n^{b/2} n^{rb/2} \log n)$, where C and r are arbitrary constants. For a default approach, given the choice of b , we set a_π exactly at $C/(p_n^{b/2} n^{rb/2} \log n)$ choosing the arbitrary constants C and r each to be 1. This is now the default choice and has been implemented in all of the examples to follow.

5 Posterior Computation

In this section we develop novel Markov chain Monte Carlo (MCMC) samplers for both the conditional and marginal R2-D2 approaches. The development of these samplers are of interest directly on their own, as after some transformation and reparametrization, we are able to obtain efficient feasible methods. In particular, the marginal version and the conditional uniform on ellipsoid version allow for fully Gibbs samplers. The conditional version with local shrinkage requires a Metropolis-Hastings sampler and we show how to sample from this posterior even in the case where $p > n$ and hence $\mathbf{X}^T \mathbf{X}$ is not full rank.

5.1 Gibbs Sampler for the Conditional Uniform-on-Ellipsoid Prior

In Proposition 2, we showed that $\boldsymbol{\beta} \mid \sigma^2$ has a mixture of normals representation for $a \leq p/2$. In practice, we recommend choosing $a = p/n$ as a default, and hence this applies as long as $n > 1$. If σ^2 is Inverse-Gamma(a_1, b_1) distributed, then $\boldsymbol{\beta}, \sigma^2, z$ and w are drawn from their full conditional distributions in the Gibbs sampler described as follows:

- (a) Set initial values for $\boldsymbol{\beta}, \sigma^2, z$ and w .

- (b) Sample $w \mid \boldsymbol{\beta}, \sigma^2, z$, by first sampling $u \sim \text{Gamma}(p/2 - a, \boldsymbol{\beta}^T \mathbf{X}^T \mathbf{X} \boldsymbol{\beta} / (2g\sigma^2))$, and setting $w = 1/(1 + u)$.
- (c) Sample $z \mid \boldsymbol{\beta}, \sigma^2, w \sim \text{Inverse-Gamma}(p/2 + b, \boldsymbol{\beta}^T \mathbf{X}^T \mathbf{X} \boldsymbol{\beta} / (2w\sigma^2) + 1/2)$.
- (d) Sample $\sigma^2 \mid \boldsymbol{\beta}, z, w \sim \text{Inverse-Gamma}((n + p)/2 + a_1, \text{SSE}/2 + \boldsymbol{\beta}^T \mathbf{X}^T \mathbf{X} \boldsymbol{\beta} / (2wz) + b_1)$, where $\text{SSE} = (\mathbf{y} - \mathbf{X}\boldsymbol{\beta})^T (\mathbf{y} - \mathbf{X}\boldsymbol{\beta})$.
- (e) Sample $\boldsymbol{\beta} \mid \sigma^2, z, w \sim \text{Normal}\left(c\widehat{\boldsymbol{\beta}}_{LS}, c\sigma^2(\mathbf{X}^T \mathbf{X})^{-1}\right)$, where $c = \frac{zw}{zw+1}$ is the shrinkage factor, and $\widehat{\boldsymbol{\beta}}_{LS}$ is the least-squares estimate of $\boldsymbol{\beta}$.
- (f) Repeat steps b-e until convergence.

5.2 MCMC for the Conditional Local Shrinkage Model

5.2.1 Full-rank case

We now develop a novel MCMC algorithm for the local shrinkage model, sampling from the full conditionals using a Metropolis-Hastings sampler. First, we take the eigen-decomposition of $\boldsymbol{\Sigma}_{\mathbf{X}} = \mathbf{X}^T \mathbf{X} / n = \mathbf{V} \mathbf{D} \mathbf{V}^T$, where $\mathbf{V}_{p \times p}$ is an orthogonal matrix of eigenvectors, and $\mathbf{D}_{p \times p}$ is a diagonal matrix of eigenvalues. R^2 is transformed such that $\theta = R^2 / (1 - R^2)$ has a Beta-Prime (or Inverted-Beta distribution), with density $p(\theta) = \theta^{a-1} (1 + \theta)^{-a-b} / B(a, b)$. We also transform $\boldsymbol{\beta}$ to lie on the unit sphere conditional on the other variables; that is, $\boldsymbol{\gamma} = \mathbf{D}^{1/2} \mathbf{V}^T \boldsymbol{\beta} / \sqrt{\theta \sigma^2}$. Then $\boldsymbol{\gamma} \mid \boldsymbol{\Lambda}$ has a Bingham distribution, and we can write the full model as follows.

$$\begin{aligned}
 \mathbf{y} \mid \boldsymbol{\gamma}, \sigma^2, \theta &\sim N_n \left(\sqrt{\theta \sigma^2} \mathbf{X} \mathbf{V} \mathbf{D}^{-1/2} \boldsymbol{\gamma}, \sigma^2 \mathbf{I} \right) \\
 \boldsymbol{\gamma} \mid \boldsymbol{\Lambda} &\sim \text{Bingham} \left(\mathbf{D}^{-1/2} \mathbf{V}^T \boldsymbol{\Lambda}^{-1} \mathbf{V} \mathbf{D}^{-1/2} \right) \\
 \sigma^2 &\sim \text{Inverse-Gamma}(a_1, b_1) \\
 \theta &\sim \text{Beta-Prime}(a, b) \\
 \lambda_j &\sim \text{Gamma}(\nu, \mu), \text{ for } j = 1, \dots, p
 \end{aligned}$$

This parametrization of the prior models the direction of $\boldsymbol{\beta}$ independently of σ^2 and R^2 . However, the Bingham distribution of the direction, $\boldsymbol{\gamma} \mid \boldsymbol{\Lambda}$, contains an intractable normalizing constant, $C_{X,\Lambda}$, depending on \mathbf{X} and $\boldsymbol{\Lambda}$. Specifically, $C_{X,\Lambda}$ is a confluent hypergeometric function with matrix argument $\mathbf{A} = \mathbf{D}^{-1/2} \mathbf{V}^T \boldsymbol{\Lambda}^{-1} \mathbf{V} \mathbf{D}^{-1/2} / 2$.

The full conditional posterior distribution of $\boldsymbol{\gamma}$ is a Fisher-Bingham($\boldsymbol{\mu}, \mathbf{A}$) distribution (Kent 1982), where $\boldsymbol{\mu} = \mathbf{y}^T \mathbf{X} \mathbf{V} \mathbf{D}^{-1/2} \sqrt{\theta / \sigma^2}$. This is equivalent to a $N_p(\mathbf{A}^{-1} \boldsymbol{\mu}, \mathbf{A}^{-1})$ distribution conditioned to lie on the $p-1$ dimensional unit sphere. We sample from this using the rejection sampler proposed by Kent et al. (2013) with an Angular Central Gaussian (ACG) envelope distribution. Sampling efficiently from the ACG distribution is possible because it is just the marginal unit direction of a multivariate Normal distribution with mean $\mathbf{0}$, and thus only requires draws from a Normal distribution. Any standard MCMC algorithm can sample θ and σ^2 , but the Adaptive Metropolis algorithm (Haario et al. 2001) automatically accounts for the strong negative correlation between the parameters without the need for manual tuning. A bivariate Normal proposal distribution is used for (σ^2, θ) with covariance proportional to the running covariance of the samples during the burn-in phase.

The density function of the full conditional posteriors for variance parameters, λ_j , almost have Generalized Inverse Gaussian distributions (GIG) if it were not for the intractable term $C_{X,\Lambda}$. A Metropolis-Hastings algorithm would require computing this quantity. Our solution is to propose each candidate λ_j^* from a GIG distribution, and introduce auxiliary variables, $\boldsymbol{\gamma}^* \mid \boldsymbol{\Lambda}^*$, from a Bingham distribution in which the constant, C_{X,Λ^*} , appears in the density. We calculate the Metropolis-Hastings acceptance probability for $(\boldsymbol{\Lambda}^*, \boldsymbol{\gamma}^*)$, and since C_{X,Λ^*} appears in the posterior and the proposal distribution, we avoid computing it. This is the so-called ‘‘Exchange Algorithm’’ proposed by Murray et al. (2006) for doubly-intractable distributions, and also used by Fallaize & Kypraios (2016) for Bayesian inference of the Bingham distribution.

The entire sampler for the local shrinkage model is described as follows:

- (a) Set initial values for $\boldsymbol{\gamma}, \sigma^2, \theta$, and $\boldsymbol{\Lambda}$.
- (b) Sample $\boldsymbol{\gamma} \mid \boldsymbol{\Lambda}$ from a Fisher-Bingham($\boldsymbol{\mu}, \mathbf{A}$) distribution, where $\boldsymbol{\mu} = \mathbf{y}^T \mathbf{X} \mathbf{V} \mathbf{D}^{-1/2} \sqrt{\theta / \sigma^2}$

and $\mathbf{A} = \mathbf{D}^{-1/2} \mathbf{V}^T \boldsymbol{\Lambda}^{-1} \mathbf{V} \mathbf{D}^{-1/2} / 2$.

(c) Sample (σ^2, θ) jointly using an Adaptive Metropolis algorithm from a bivariate Normal distribution.

(d) Exchange algorithm to sample $\boldsymbol{\Lambda}$:

(i) Sample $\lambda_j^* \mid u_j \sim \text{GIG}(\nu, 2\mu, u_j^2)$, for $j = 1, \dots, p$, where $\mathbf{u} = \mathbf{V} \mathbf{D}^{-1/2} \boldsymbol{\gamma}$.

(ii) Sample \mathbf{u}^* from a Bingham(\mathbf{A}^*) distribution, where $\mathbf{A}^* = \mathbf{D}^{-1/2} \mathbf{V}^T \boldsymbol{\Lambda}^{*-1} \mathbf{V} \mathbf{D}^{-1/2} / 2$

(iii) Accept $(\boldsymbol{\Lambda}^*, \mathbf{u}^*)$ with probability:

$$\frac{p(\boldsymbol{\Lambda}^* | \mathbf{u})}{p(\boldsymbol{\Lambda} | \mathbf{u})} \times \frac{q(\boldsymbol{\Lambda} | \mathbf{u})}{q(\boldsymbol{\Lambda}^* | \mathbf{u})} \times \frac{q(\mathbf{u}^* | \boldsymbol{\Lambda})}{q(\mathbf{u}^* | \boldsymbol{\Lambda}^*)} = \exp \left\{ \sum_{j=1}^p u_j^{*2} (1/\lambda_j^{*2} - 1/\lambda_j^2) \right\}$$

(e) Repeat steps (b)-(d) until convergence, and calculate $\boldsymbol{\beta} = \sqrt{\theta \sigma^2} \mathbf{V} \mathbf{D}^{-1/2} \boldsymbol{\gamma}$ for each sample.

In step (d), $p(\boldsymbol{\Lambda} \mid \mathbf{u})$ is the conditional posterior distribution of $\boldsymbol{\Lambda}$; $q(\boldsymbol{\Lambda} \mid \mathbf{u})$ is the GIG proposal distribution with density: $p(x; d, a, b) \propto x^{d-1} \exp \{ -(ax + b/x)/2 \}$, for $-\infty < d < \infty$, and $a, b > 0$; and $q(\mathbf{u} \mid \boldsymbol{\Lambda})$ is the Bingham proposal distribution which has the same constant as in $p(\boldsymbol{\Lambda} \mid \mathbf{u})$. We only need to keep $\boldsymbol{\Lambda}^*$ at each step, and can discard \mathbf{u}^* . We can efficiently sample from the Bingham distribution because it is a special case of the Fisher-Bingham with $\boldsymbol{\mu} = \mathbf{0}$ (Kent et al. 2013). All modeling is done in terms of $\boldsymbol{\gamma}, \sigma^2, \theta$ and $\boldsymbol{\Lambda}$, and we calculate $\boldsymbol{\beta}$ outside the sampler.

5.2.2 Non full-rank case

Next we address how to fit these models with high-dimensional data, where $p > n$ and $\mathbf{X}^T \mathbf{X}$ is not full rank. The restriction on $\boldsymbol{\beta} : \boldsymbol{\beta}^T \boldsymbol{\Sigma}_{\mathbf{X}} \boldsymbol{\beta} = \sigma^2 \theta$, is no longer an ellipsoid, but an unbounded subspace in p -dimensions (e.g. parallel lines for $p = 2$, and an infinite cylinder for $p = 3$). We assume that the $\text{rank}(\mathbf{X}) = n$, and partition $\mathbf{D} = \begin{pmatrix} \mathbf{D}_1 & \mathbf{0} \\ \mathbf{0} & \mathbf{0} \end{pmatrix}$ and $\mathbf{V} = (\mathbf{V}_1, \mathbf{V}_2)$. Note that \mathbf{D}_1 is the $n \times n$ diagonal matrix of positive eigenvalues, \mathbf{V}_1 is the matrix of corresponding eigenvectors, and \mathbf{V}_2 is the matrix of the $p-n$ eigenvectors spanning the null space of \mathbf{X} . We define $\boldsymbol{\gamma} = (\boldsymbol{\gamma}_1, \boldsymbol{\gamma}_2)^T = (\mathbf{D}_1^{1/2} \mathbf{V}_1^T \boldsymbol{\beta}, \mathbf{V}_2^T \boldsymbol{\beta})^T / \sqrt{\theta \sigma^2}$, so that $\boldsymbol{\gamma}$ is

multivariate Normal with the constraint that $\boldsymbol{\gamma}_1^T \boldsymbol{\gamma}_1 = 1$. Marginally, $\boldsymbol{\gamma}_1 = \mathbf{D}_1^{1/2} \mathbf{V}_1^T \boldsymbol{\beta} / \sqrt{\theta \sigma^2}$ is defined on the $n - 1$ dimensional unit sphere, and has a Fisher-Bingham distribution just like the full rank case. However, the reverse transformation $\boldsymbol{\beta} = \sqrt{\theta \sigma^2} \mathbf{V}_1 \mathbf{D}_1^{-1/2} \boldsymbol{\gamma}_1$ is defined on the lower $n - 1$ dimensional ellipsoid within the entire constrained space $\{\boldsymbol{\beta} : \boldsymbol{\beta}^T \boldsymbol{\Sigma}_X \boldsymbol{\beta} = \sigma^2 \theta\}$. For example, if $p = 3$ and $n = 2$, this is the slice of the 3-dimensional ellipsoid with the minimum L_2 -norm. The problem is that this lower dimensional ellipsoid may not be able to favor the sparsity or local shrinkage encouraged by $\boldsymbol{\Lambda}$. That would be equivalent to principal components regression using the top n principal components. To allow for shrinkage of the original coefficients and not the principal components, we sample $\boldsymbol{\gamma}_2 \mid \boldsymbol{\gamma}_1$, which is multivariate Normal, and make the reverse transformation $\boldsymbol{\beta} = \sqrt{\theta \sigma^2} \left(\mathbf{V}_1 \mathbf{D}_1^{-1/2} \boldsymbol{\gamma}_1 + \mathbf{V}_2 \boldsymbol{\gamma}_2 \right)$. Since \mathbf{V}_2 spans the null space of \mathbf{X} , $\boldsymbol{\beta}$ is still in the constrained region, but offers more flexibility in shrinking β_j .

5.3 Gibbs Sampler for Marginal R2-D2

For posterior computation in the marginal case, the following equivalent representation is useful. The R2-D2 prior (8) is equivalent to

$$\begin{aligned} \beta_j \mid \sigma^2, \psi_j, \phi_j, \omega &\sim N(0, \psi_j \phi_j \omega \sigma^2 / 2), \quad \psi_j \sim \text{Exp}(1/2), \\ \phi &\sim \text{Dir}(a_\pi, \dots, a_\pi), \quad \omega \mid \xi \sim \text{Ga}(a, \xi), \quad \xi \sim \text{Ga}(b, 1), \end{aligned} \quad (13)$$

where $\text{Exp}(\delta)$ denotes the exponential distribution with mean δ^{-1} . The Gibbs sampling procedure is based on (13) with $a = pa_\pi$. Denote $Z \sim \text{InvGaussian}(\mu, \lambda)$, if $\pi(z) = \lambda^{1/2} (2\pi z^3)^{-1/2} \exp\{-\lambda(z - \mu)^2 / (2\mu^2 z)\}$. Denote $Z \sim \text{giG}(\chi, \rho, \lambda_0)$, the generalized inverse Gaussian distribution (Seshadri 1997), if $\pi(z) \propto z^{\lambda_0 - 1} \exp\{-(\rho z + \chi/z)/2\}$.

The Gibbs sampling procedure is as follows:

- (a) Set initial values for $\boldsymbol{\beta}, \sigma^2, \boldsymbol{\psi}, \boldsymbol{\phi}$, and ω .
- (b) Sample $\boldsymbol{\beta} \mid \boldsymbol{\psi}, \boldsymbol{\phi}, \omega, \sigma^2, \mathbf{Y} \sim N(\boldsymbol{\mu}, \sigma^2 \mathbf{V})$, where $\boldsymbol{\mu} = \mathbf{V} \mathbf{X}^T \mathbf{Y} = (\mathbf{X}^T \mathbf{X} + \mathbf{S}^{-1})^{-1} (\mathbf{X}^T \mathbf{Y})$, $\mathbf{V} = (\mathbf{X}^T \mathbf{X} + \mathbf{S}^{-1})^{-1}$, $\mathbf{S} = \text{diag}\{\psi_1 \phi_1 \omega / 2, \dots, \psi_p \phi_p \omega / 2\}$, $\mathbf{X} = (\mathbf{x}_1, \dots, \mathbf{x}_n)^T$, and $\mathbf{Y} = (Y_1, \dots, Y_n)^T$.

- (c) Sample $\sigma^2 \mid \boldsymbol{\beta}, \boldsymbol{\psi}, \boldsymbol{\phi}, \omega, \mathbf{Y} \sim \text{IG}(a_1 + (n + p)/2, b_1 + (\boldsymbol{\beta}^T \mathbf{S}^{-1} \boldsymbol{\beta} + (\mathbf{Y} - \mathbf{X}\boldsymbol{\beta})^T (\mathbf{Y} - \mathbf{X}\boldsymbol{\beta}))/2)$.
- (d) Sample $\boldsymbol{\psi} \mid \boldsymbol{\beta}, \boldsymbol{\phi}, \omega, \sigma^2$. Draw $\psi_j^{-1} \sim \text{InvGaussian}(\mu_j = \sqrt{\sigma^2 \phi_j \omega / 2} / |\beta_j|, \lambda = 1)$, then take the reciprocal to get ψ_j .
- (e) Sample $\omega \mid \boldsymbol{\beta}, \boldsymbol{\psi}, \boldsymbol{\phi}, \xi, \sigma^2 \sim \text{giG}(\chi = \sum_{j=1}^p 2\beta_j^2 / (\sigma^2 \psi_j \phi_j), \rho = 2\xi, \lambda_0 = a - p/2)$.
- (f) Sample $\xi \mid \omega \sim \text{Ga}(a + b, 1 + \omega)$.
- (g) Sample $\boldsymbol{\phi} \mid \boldsymbol{\beta}, \boldsymbol{\psi}, \xi, \sigma^2$. Motivated by Bhattacharya et al. (2015), if $a = pa_\pi$, one can draw T_1, \dots, T_p independently with $T_j \sim \text{giG}(\chi = 2\beta_j^2 / (\sigma^2 \psi_j), \rho = 2\xi, \lambda_0 = a_\pi - 1/2)$. Then set $\phi_j = T_j / T$ with $T = \sum_{j=1}^p T_j$.
- (h) Repeat steps (b)-(g) until convergence.

6 Simulation Study

We conduct a simulation study to compare the proposed approach with other Bayesian regression models. In each setting, 200 datasets are simulated from the homoscedastic linear model (1), with sample size $n = 60$, and the number of predictors p varying in $p \in \{50, 100, 500, 2000\}$. Larger sample sizes were also investigated with the comparisons remaining similar. The covariates $\mathbf{x}_i, i = 1, \dots, n$, are generated from multivariate normal distribution with mean zero, and correlation matrix of autoregressive structure AR(1) with correlation $\rho = 0.5$ or 0.9 . For the regression coefficients $\boldsymbol{\beta}$, we set $\boldsymbol{\beta} = (\mathbf{0}_{10}^T, \mathbf{B}_1^T, \mathbf{0}_{30}^T, \mathbf{B}_2^T, \mathbf{0}_{p-50}^T)^T$ with $\mathbf{0}_k$ representing the zero vector of length k , and \mathbf{B}_1 and \mathbf{B}_2 each of length 5 nonzero elements. The fractions of true coefficients with exactly zero values are 80%, 90%, 98%, and 99.5% for $p \in \{50, 100, 500, 2000\}$, respectively, and the remaining 20%, 10%, 2%, and 0.5% nonzero elements \mathbf{B}_1 and \mathbf{B}_2 were independently generated from two scenarios: (i) a Student t distribution with 3 degrees of freedom to give heavy tails; (ii) a Uniform(0,1) distribution to give weaker signals. For scenario (i), we set the error variance to produce a Signal-to-Noise Ratio (SNR) of 9, yielding $\sigma^2 = 10/3$. Note

that since the generated coefficients have expectation of zero, the SNR does not depend on the correlation structure of the covariates. For scenario (ii), the nonzero expectation of the Uniform(0,1) then entails a different SNR for the 2 different correlation setups. For this scenario, we set $\sigma^2 = 6$ to yield SNR ≈ 0.5 and 0.7 in the $\rho = 0.5$ and 0.9 cases, respectively.

To implement both the marginal and conditional R2-D2 priors, as discussed as a default choice in Section 4.2.4, we set $b = 0.5$ to yield Cauchy-like tails, and $a_\pi = C/(p_n^{b/2} n^{rb/2} \log n)$ with choosing the arbitrary constants C and r to be 1. We also set $b = 0.1$ to give heavier tails (then setting a_π in the same manner). The results for $b = 0.1$ were similar to $b = 0.5$ and thus not shown, and we recommend as a default to use $b = 0.5$ as a fully automatic approach. For the conditional R2-D2, the choices of ν and μ in the Gamma prior are based on the recommendations for implementation of Normal-Gamma priors given in Griffin & Brown (2010). The choice is based on the degree of sparsity, which we choose as $\min\{n, 0.1p\}$ so that we set the expected number of non-zero coefficients to be 10% of the total, or the sample size, whichever is smaller. Details of how ν and μ relate to the sparsity level are given in the Appendix.

The comparisons are made to some current state-of-the-art global-local priors: Horseshoe, Horseshoe+, Normal-Beta Prime and Dirichlet-Laplace.

For the Horseshoe, Dirichlet-Laplace, and Normal-Beta Prime, the implementation is done via the R packages `horseshoe`, `dlbayes`, and `NormalBetaPrime`, respectively. The Horseshoe+ is implemented through `Stan` in R using the code provided by the author of Bhadra et al. (2016). The proposed R2-D2 approaches are implemented in R, based on the discussed MCMC sampling.

In all cases, 10,000 samples are collected with the first 5,000 samples discarded as burn-in.

Estimation error and AUC. The average sum of squared error corresponding to the posterior mean across the 200 replicates is provided in Table 2 for simulation setting i for $p = 100$ and 500 and in Table 3 for simulation setting ii. In addition, the averaged area under the Receiver-Operating Characteristic (ROC) curve (AUC) based on the posterior

t -statistic, i.e., the ratio of the posterior mean and posterior standard deviation, is also given to offer further evaluation of the reliability of the posterior inference on the coefficients. Larger AUC signifies that the method tends to give posterior intervals further away from zero for the true non-zero coefficients and intervals that are concentrated closer to zero for the irrelevant variables. To perform variable selection, thresholding the posteriors either marginally or jointly (Bondell & Reich 2012) is typical, and thus higher AUC would represent more accurate variable selection.

	Scenario 1 [non-zero coefficients from t_3]							
	$\rho = 0.5$				$\rho = 0.9$			
	p=100		p=500		p=100		p=500	
	SSE	AUC	SSE	AUC	SSE	AUC	SSE	AUC
Horseshoe	148 (6.4)	64	236 (13.1)	61	186 (9.2)	67	205 (11.2)	68
Horseshoe+	146 (5.8)	64	215 (11.4)	62	190 (9.7)	67	212 (11.4)	69
Normal-BetaPrime	155 (5.7)	64	578 (20.1)	59	183 (8.1)	67	1399 (62.1)	57
Dirichlet-Laplace	166 (7.8)	67	187 (8.1)	54	197 (11.6)	74	209 (10.9)	59
R2-D2 - Conditional	146 (5.6)	66	179 (7.9)	62	174 (8.1)	73	192 (11.2)	72
R2-D2 - Marginal	142 (5.5)	65	166 (6.5)	64	179 (8.7)	72	188 (10.1)	73

Table 2: Average sum of squared error (SSE) and average area under the Receiver-Operating Characteristic curve (AUC), based on 200 simulated datasets. All values multiplied by 10 for readability. For SSE, standard errors are included in parentheses. For AUC, all standard errors are in the range of 0.5 – 0.7, so omitted to save space. Note that *smaller* is better for SSE, while *larger* is better for AUC. Best performance in each column is highlighted in bold for reference.

It is clear from Table 2 and 3 that the proposed approaches, both conditional and marginal R2-D2 prior, outperform the existing methods in nearly every case, both in terms of the estimation error, and the area under the ROC curve. This is particularly apparent in the cases of $p = 500$. The Dirichlet-Laplace performs well in some of the cases with $p = 100$, but then performs significantly worse with $p = 500$, particularly in AUC. Both the conditional and marginal versions of R2-D2 prior perform similarly, with slightly better performance of the conditional version in the lower dimensional case, but slightly better performance of the marginal version in the case of $p = 500$. Overall, the proposed approach

	Scenario 2 [non-zero coefficients from U(0,1)]							
	$\rho = 0.5$				$\rho = 0.9$			
	p=100		p=500		p=100		p=500	
	SSE	AUC	SSE	AUC	SSE	AUC	SSE	AUC
Horseshoe	44.1 (1.9)	62	59.9 (4.8)	58	41.7 (2.2)	73	39.8 (3.2)	58
Horseshoe+	47.0 (2.2)	62	79.2 (8.1)	61	47.6 (4.2)	73	44.9 (4.4)	63
Normal-BetaPrime	62.4 (2.4)	62	437.1 (14.2)	57	42.5 (1.7)	70	1203 (55.1)	59
Dirichlet-Laplace	32.4 (0.7)	64	56.3 (5.7)	51	27.3 (0.6)	79	41.3 (1.2)	64
R2-D2 - Conditional	34.5 (1.2)	66	48.2 (2.9)	59	26.3 (0.6)	82	38.1 (1.7)	79
R2-D2 - Marginal	33.7 (1.0)	64	41.0 (1.3)	65	31.8 (1.2)	76	34.5 (1.0)	82

Table 3: Average sum of squared error (SSE) and average area under the Receiver-Operating Characteristic curve (AUC), based on 200 simulated datasets. All values multiplied by 10 for readability. For SSE, standard errors are included in parentheses. For AUC, all standard errors are in the range of 0.5 – 0.7, so omitted to save space. Note that *smaller* is better for SSE, while *larger* is better for AUC. Best performance in each column is highlighted in bold for reference.

gives a much improved result over the existing approaches. This is to be anticipated based on the theoretical results on the concentration and tail behaviors, which we now examine.

To better understand the relative performance of the methods, Table 4 shows the average SSE partitioned according to the value of the true β at $\beta_j = 0$, $|\beta_j| \in (0, 0.5]$, and $|\beta_j| > 0.5$, $j = 1, \dots, p$. This allows us to view a more detailed performance of the approaches in their behavior on the zero, small non-zero, and larger non-zero coefficients, respectively. The table shows the results for $\rho = 0.5$ and $p = 100$ for setting i, but the decomposed SSE is similar in the other cases as well.

From the breakdown provided in Table 4, we see the differences between the approaches, and the theoretical results on the concentration at zero and tail behavior (Table 1) really show up strongly here. Since the Dirichlet-Laplace has high concentration around zero, but it has tails that are much lighter than the others, we see this translate into really small error on the zero and small coefficients, but extremely large error on the large coefficients. Meanwhile, the Horseshoe and Horseshoe+ having less concentration around zero leads to poorer performance at estimation of the actual zeros. Note that this also explains the

	$\beta = 0$	$ \beta \in (0, 0.5]$	$ \beta > 0.5$	Total
Horseshoe	21	24	103	148
Horseshoe+	18	22	106	146
Normal-BetaPrime	35	38	82	155
Dirichlet-Laplace	4	6	156	166
R2D2 - Conditional	14	18	114	146
R2D2 - Marginal	10	13	119	142

Table 4: Average sum of squared error broken down by zero coefficients ($\beta = 0$), small coefficients ($|\beta| \in (0, 0.5]$), large coefficients ($|\beta| > 0.5$), and Total. Results are based on the 200 datasets from Table 2 with $p = 100$ and $\rho = 0.5$.

reason for the Horseshoe and Horseshoe+ having worse AUC, as it does not push the zeros close enough to zero in order to distinguish them from the small coefficients. Note that the R2-D2 was set with $b = 0.5$ giving it the Cauchy-like tails as is the case with the Horseshoe. Thus we see similar estimation ability for the larger coefficients. Overall, the proposed R2-D2 approach achieves a strong performance in both regions simultaneously as anticipated by the theory.

Credible Interval Coverage. We also examine the coverage properties of using 95% marginal credible intervals for each approach. For this same scenario, table 5 reports the average width of the intervals, the proportion of coverage, the Specificity, and the Sensitivity. This gives a broader picture of the posterior inference properties. Although, there is no promise of 95% Frequentist coverage by the 95% intervals, we see that in this case of $n = 60$ and $p = 100$, the coverage of most of the approaches are close to 95%, with the proposed approaches and the Horseshoe+ being almost right on the value, while the Horseshoe and DL are a bit lower than the target, and the NBP being a bit large. For the $n = 60$ case, this is a very difficult problem even when $p = 100$, and we see that the sensitivity (power) for all approaches are quite low due to the intervals containing zero even for the majority of the true non-zeros. The sensitivity for the R2-D2 approaches are highest, along with the Horseshoe+ and Normal-Beta Prime. However, in order to do so, the Horseshoe+ and Normal-Beta Prime intervals are quite wide in comparison, thus

showing that our proposed approaches look to have good posterior inference properties in addition to their outstanding performance in estimation and variable importance ordering.

	Avg Width	Coverage	Sensitivity	Specificity
Horseshoe	0.81	0.936	0.190	0.999
Horseshoe+	1.23	0.953	0.310	0.999
Normal-BetaPrime	1.83	0.972	0.301	0.999
Dirichlet-Laplace	0.91	0.939	0.150	1
R2D2 - Conditional	0.98	0.947	0.350	0.999
R2D2 - Marginal	1.11	0.948	0.290	1

Table 5: Coverage properties of 95% marginal posterior credible intervals. Results are based on the 200 datasets from Table 2 with $p = 100$ and $\rho = 0.5$.

Higher dimensional setting. Table 6 shows the results for $p = 2000$ and $n = 60$ for scenario i with $\rho = 0.5$. Other settings are similar and hence not shown. Table 6 shows the estimation error and AUC as before. We also include coverage of the 95% intervals, and also the coverage on only the non-zero coefficients. For estimation and AUC, we again see that the performance of the proposed R2-D2 approaches perform very well in this higher dimensional case.

In terms of coverage of the 95% intervals, as shown in van der Pas et al. (2017b) (Theorems 1 and 2), for the HS credible intervals in the special case of the Normal means model, the coverage will either go to zero or one depending on the size of the true coefficient. We see that in this case of $p = 2000$ and $n = 60$, all methods have overall coverage of nearly 100%. However, stark differences appear in looking at the coverage on the non-zero coefficients only (of which there are only 10 out of 2000 here). We see that the HS, in particular, almost never covers these non-zero values, with coverage of 1.5% (HS) or 5% (HS+). This is anticipated by the results of van der Pas et al. (2017b) given that it attempts to adapt to the sparsity, thus covering the zeros, at the expense of the non-zeros. We see that the other methods do better at coverage of the non-zeros here (with the marginal R2-D2 way up at 47%). We see in this higher dimensional case, the proposed approaches exhibiting more stability, both in estimation error, and in the coverage.

	$p = 2000, n = 60$ [non-zero coefficients from t_3]			
	SSE	AUC	Coverage	Coverage on non-zeros
Horseshoe	249 (9.6)	44	0.995	0.015
Horseshoe+	233 (8.9)	51	0.996	0.050
Normal-BetaPrime	468 (15.7)	61	0.995	0.240
Dirichlet-Laplace	240 (8.7)	56	0.996	0.165
R2D2 - Conditional	201 (7.1)	65	0.996	0.271
R2D2 - Marginal	196 (6.9)	64	0.997	0.466

Table 6: Simulation setting 1 with $p = 2000$, $n = 60$, and $\rho = 0.5$. Average sum of squared error (with standard error), area under the ROC curve, overall coverage of 95% credible intervals on all 2000 coefficients, and coverage of the 95% credible intervals on the 10 non-zero coefficients only. Results are based on 200 datasets.

7 Data Examples

We study the predictive performance of the posterior generated by the R2-D2 prior through a variety of real examples which exhibit varying structures. These three data sets have many more parameters than observations, and have very different correlation structures. The Cereal data consists of starch content measurements from 15 observations with 145 infrared spectra measurements as predictors. The data is provided with the `chemometrics` R package. The Cookie data arises from an experiment testing the near-infrared (NIR) spectroscopy of biscuit dough in which the fat content is measured on 72 samples, with 700 NIR spectra measurements as predictors. The data was generated in the experiment by Osborne et al. (1984), and is available in the `pp1s` R package. The Multidrug data are from a pharmacogenomic study investigating the relationship between the drug concentration (at which 50% growth is inhibited for a human cell line) and expression of the adenosine triphosphate binding cassette transporter (Szakács et al. 2004). The data consists of 853 drugs as predictors, 60 samples of human cell lines using the ABCA3 transporter as the response, and is available in the `mixOmics` R package. In the statistics literature, the Cereal and Multidrug data were both studied by Polson & Scott (2012) and Griffin & Brown (2013); and the Cookie data was studied by Brown et al. (2001) and Ghosh &

Ghattas (2015).

The three datasets nicely represent 3 different correlation structures among the predictor variables. The Multidrug covariates have low to moderate pairwise correlations, the Cookie covariates are highly positively correlated, and the Cereal covariates have a wide range that are both positively and negatively correlated. Figure 3 shows histograms of all pairwise correlations for each of the data sets.

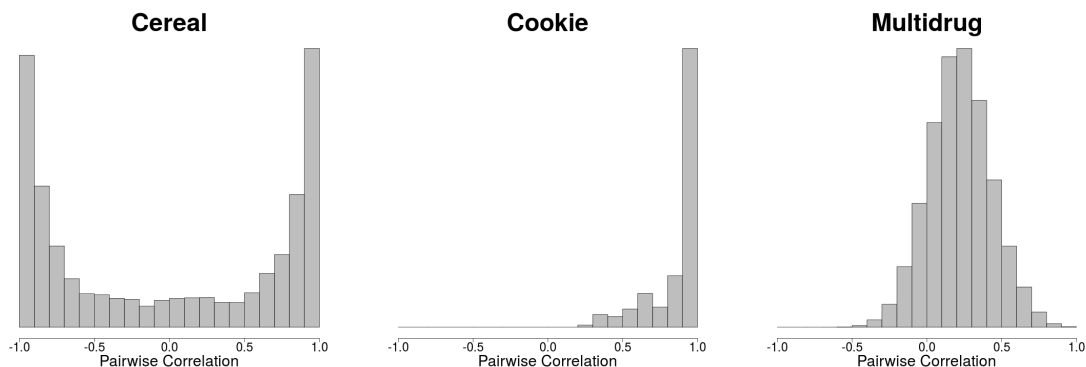


Figure 3: Histograms of pairwise correlations among the predictor variables for the three datasets.

	Cereal	Cookie	Multidrug
n	15	72	60
p	145	700	853
Horseshoe	14.1 (1.0)	8.3 (0.2)	15.6 (0.5)
Horseshoe+	14.2 (0.9)	9.1 (0.3)	15.0 (0.5)
Normal-BetaPrime	25.4 (1.5)	11.9 (0.4)	18.4 (0.6)
Dirichlet-Laplace	15.1 (1.2)	12.1 (0.5)	12.2 (0.3)
R2-D2 - Conditional	12.2 (0.5)	9.8 (0.3)	12.7 (0.3)
R2-D2 - Marginal	12.1 (0.5)	8.1 (0.2)	12.6 (0.3)

Table 7: Average mean square prediction error (and standard errors) for each of the data examples.

We randomly split each data set into a training and testing sets to evaluate the out-of-sample predictive performance. For each data set, 75% of the observations were used for training, and the remaining 25% were used for estimating the mean squared prediction

error (MSPE) between the test sample and predictions. This process was repeated to create 200 data sets for each example. The same 5 approaches as in the simulations were used on each of the datasets. Due to the various correlation structures and dimensions, this gives a range of potential data structures for comparison of the approaches.

The average MSPE results are given in Table 7. We see that the R2-D2 approaches consistently outperform the existing methods across the datasets. Note that the Horseshoe and Horseshoe+ perform well on the Cookie data, but are significantly worse than the others on the other 2 datasets.

8 Discussion

In this paper, we propose a shrinkage prior motivated by assuming a prior on R^2 . The prior exhibits polynomial behavior both around the origin and in the tails and compares favorably with other global-local shrinkage priors. Although the motivation of our R2-D2 prior is via starting with a prior on R^2 , the resultant prior is simply a member of the class of global-local shrinkage priors, which can then be applied directly to other models, as with other priors. The prior is represented by a hierarchical scale mixture of normals, which can then be implemented in a generalized linear model or other regression setting. The hyperparameters would no longer have the interpretation as parameters of a Beta prior on the R^2 of the model. But the form and properties of the resulting prior, such as tail behavior and concentration around zero remain directly useable as is with the other global-local priors.

There is scope for further advances in algorithms for MCMC sampling for these posteriors, just as there has been for sampling from other prior proposals, as for example, key sampling approaches for the high-dimensional case as in Bhattacharya et al. (2016).

References

Armagan, A., Clyde, M. & Dunson, D. B. (2011), Generalized beta mixtures of Gaussians, *in* ‘Advances in neural information processing systems’, pp. 523–531.

- Armagan, A., Dunson, D. B. & Lee, J. (2013), ‘Generalized double Pareto shrinkage’, *Statistica Sinica* **23**(1), 119.
- Armagan, A., Dunson, D. B., Lee, J., Bajwa, W. U. & Strawn, N. (2013), ‘Posterior consistency in linear models under shrinkage priors’, *Biometrika* **100**(4), 1011–1018.
- Bai, R. & Ghosh, M. (2019), ‘Large-scale multiple hypothesis testing with the normal-beta prime prior’, *Statistics* **53**(6), 1210–1233.
- Bateman, H. (1953), *Higher Transcendental Functions [Volumes I-III]*, Vol. 1, McGraw-Hill Book Company.
- Bhadra, A., Datta, J., Polson, N. G. & Willard, B. (2016), ‘The horseshoe+ estimator of ultra-sparse signals’, *Bayesian Analysis* .
- Bhattacharya, A., Chakraborty, A. & Mallick, B. (2016), ‘Fast sampling with gaussian scale-mixture priors in high-dimensional regression’, *Biometrika* **103**(4), 985–991.
- Bhattacharya, A., Pati, D., Pillai, N. S. & Dunson, D. B. (2015), ‘Dirichlet–laplace priors for optimal shrinkage’, *Journal of the American Statistical Association* **110**(512), 1479–1490.
- Bingham, C. (1974), ‘An antipodally symmetric distribution on the sphere’, *The Annals of Statistics* pp. 1201–1225.
- Bondell, H. D. & Reich, B. J. (2012), ‘Consistent high-dimensional bayesian variable selection via penalized credible regions’, *Journal of the American Statistical Association* **107**(500), 1610–1624.
- Brown, P. J., Fearn, T. & Vannucci, M. (2001), ‘Bayesian wavelet regression on curves with application to a spectroscopic calibration problem’, *Journal of the American Statistical Association* **96**(454), 398–408.
- Carvalho, C. M., Polson, N. G. & Scott, J. G. (2009), Handling sparsity via the horseshoe, *in* ‘International Conference on Artificial Intelligence and Statistics’, pp. 73–80.

- Carvalho, C. M., Polson, N. G. & Scott, J. G. (2010), ‘The Horseshoe estimator for sparse signals’, *Biometrika* **97**, 465–480.
- Castillo, I., Schmidt-Hieber, J. & van der Vaart, A. (2015), ‘Bayesian linear regression with sparse priors’, *The Annals of Statistics* **43**(5), 1986–2018.
- DLMF (2015), ‘NIST Digital Library of Mathematical Functions’, <http://dlmf.nist.gov/>, Release 1.0.10 of 2015-08-07. Online companion to Olver et al. (2010).
URL: <http://dlmf.nist.gov/>
- Fallaize, C. J. & Kypraios, T. (2016), ‘Exact bayesian inference for the bingham distribution’, *Statistics and Computing* **26**(1-2), 349–360.
- Fields, J. L. (1972), ‘The asymptotic expansion of the Meijer G-function’, *Mathematics of Computation* pp. 757–765.
- George, E. I. & McCulloch, R. E. (1993), ‘Variable selection via Gibbs sampling’, *Journal of the American Statistical Association* **88**(423), 881–889.
- Ghosh, J. & Ghattas, A. E. (2015), ‘Bayesian variable selection under collinearity’, *The American Statistician* **69**(3), 165–173.
- Griffin, J. E. & Brown, P. J. (2010), ‘Inference with normal-gamma prior distributions in regression problems’, *Bayesian Analysis* **5**(1), 171–188.
- Griffin, J. E. & Brown, P. J. (2013), ‘Some priors for sparse regression modelling’, *Bayesian Analysis* **8**(3), 691–702.
- Haario, H., Saksman, E. & Tamminen, J. (2001), ‘An adaptive metropolis algorithm’, *Bernoulli* pp. 223–242.
- Hans, C., Dobra, A. & West, M. (2007), ‘Shotgun stochastic search for large p regression’, *Journal of the American Statistical Association* **102**(478), 507–516.
- Ishwaran, H. & Rao, J. S. (2005), ‘Spike and slab variable selection: Frequentist and Bayesian strategies’, *Annals of Statistics* pp. 730–773.

- Johnson, N., Kotz, S. & Balakrishnan, N. (1995), ‘Continuous univariate distributions, volume 2. john wiley&sons’, *Inc.*, **75**.
- Kent, J. T. (1982), ‘The fisher-bingham distribution on the sphere’, *Journal of the Royal Statistical Society. Series B (Methodological)* pp. 71–80.
- Kent, J. T., Ganeiber, A. M. & Mardia, K. V. (2013), ‘A new method to simulate the bingham and related distributions in directional data analysis with applications’, *arXiv preprint arXiv:1310.8110* .
- Miller, P. D. (2006), *Applied asymptotic analysis*, Vol. 75, American Mathematical Soc.
- Mitchell, T. J. & Beauchamp, J. J. (1988), ‘Bayesian variable selection in linear regression’, *Journal of the American Statistical Association* **83**(404), 1023–1032.
- Murray, I., Ghahramani, Z. & MacKay, D. (2006), Mcmc for doubly-intractable distributions, *in* ‘Proceedings of the 22nd annual conference on uncertainty in artificial intelligence’, AUAI Press, pp. 359–366.
- Narisetty, N. N. & He, X. (2014), ‘Bayesian variable selection with shrinking and diffusing priors’, *The Annals of Statistics* **42**(2), 789–817.
- Olver, F. W. J., Lozier, D. W., Boisvert, R. F. & Clark, C. W., eds (2010), *NIST Handbook of Mathematical Functions*, Cambridge University Press, New York, NY. Print companion to DLMF (2015).
- Ormerod, J. T., You, C. & Müller, S. (2017), ‘A variational bayes approach to variable selection’, *Electronic Journal of Statistics* **11**(2), 3549–3594.
- Osborne, B. G., Fearn, T., Miller, A. R. & Douglas, S. (1984), ‘Application of near infrared reflectance spectroscopy to the compositional analysis of biscuits and biscuit doughs’, *Journal of the Science of Food and Agriculture* **35**(1), 99–105.
- Polson, N. G. & Scott, J. G. (2010), ‘Shrink globally, act locally: Sparse bayesian regularization and prediction’, *Bayesian Statistics* **9**, 501–538.

- Polson, N. G. & Scott, J. G. (2012), ‘Local shrinkage rules, lévy processes and regularized regression’, *Journal of the Royal Statistical Society: Series B (Statistical Methodology)* **74**(2), 287–311.
- Raskutti, G., Wainwright, M. J. & Yu, B. (2011), ‘Minimax rates of estimation for high-dimensional linear regression over ℓ_q -balls’, *IEEE transactions on information theory* **57**(10), 6976–6994.
- Ročková, V. & George, E. I. (2014), ‘Emvs: The em approach to bayesian variable selection’, *Journal of the American Statistical Association* **109**(506), 828–846.
- Ročková, V. & George, E. I. (2018), ‘The spike-and-slab lasso’, *Journal of the American Statistical Association* **113**(521), 431–444.
- Scott, S. L. & Varian, H. R. (2014), ‘Predicting the present with bayesian structural time series’, *International Journal of Mathematical Modelling and Numerical Optimisation* **5**(1-2), 4–23.
- Seshadri, V. (1997), ‘Halphen’s laws’, *Encyclopedia of statistical sciences* .
- Song, Q. & Liang, F. (2017), ‘Nearly optimal bayesian shrinkage for high dimensional regression’, *arXiv preprint arXiv:1712.08964* .
- Szakács, G., Annereau, J.-P., Lababidi, S., Shankavaram, U., Arciello, A., Bussey, K. J., Reinhold, W., Guo, Y., Kruh, G. D. & Reimers, M. (2004), ‘Predicting drug sensitivity and resistance: profiling abc transporter genes in cancer cells’, *Cancer cell* **6**(2), 129–137.
- van der Pas, S. L., Kleijn, B. J. & van der Vaart, A. W. (2014), ‘The horseshoe estimator: Posterior concentration around nearly black vectors’, *Electronic Journal of Statistics* **8**(2), 2585–2618.
- van der Pas, S., Szabó, B. & van der Vaart, A. (2017a), ‘Adaptive posterior contraction rates for the horseshoe’, *Electronic Journal of Statistics* **11**(2), 3196–3225.

- van der Pas, S., Szabó, B. & van der Vaart, A. (2017b), ‘Uncertainty quantification for the horseshoe (with discussion)’, *Bayesian Analysis* **12**(4), 1221–1274.
- Zellner, A. & Siow, A. (1980), ‘Posterior odds ratios for selected regression hypotheses’, *Trabajos de estadística y de investigación operativa* **31**(1), 585–603.
- Zhang, Y. & Bondell, H. D. (2018), ‘Variable selection via penalized credible regions with dirichlet–laplace global-local shrinkage priors’, *Bayesian Analysis* **13**(3), 823–844.
- Zhou, M. & Carin, L. (2015), ‘Negative binomial process count and mixture modeling’, *Pattern Analysis and Machine Intelligence, IEEE Transactions on* **37**(2), 307–320.
- Zwillinger, D. (2014), *Table of integrals, series, and products*, Elsevier.

A Appendix: Technical Details

Definition of the Meijer G-function.

A general definition of the Meijer G-function is given by the following line integral in the complex plane (Bateman 1953):

$$G_{p,q}^{m,n} \left(z \left| \begin{matrix} a_1, \dots, a_p \\ b_1, \dots, b_q \end{matrix} \right. \right) = \frac{1}{2\pi i} \int_L \frac{\prod_{j=1}^m \Gamma(b_j - s) \prod_{j=1}^n \Gamma(1 - a_j + s)}{\prod_{j=m+1}^q \Gamma(1 - b_j + s) \prod_{j=n+1}^p \Gamma(a_j - s)} z^s ds$$

where $\Gamma(\cdot)$ denotes the gamma function and L in the integral represents the path to be followed while integrating. The definition holds under the following assumptions:

- $0 \leq m \leq q$ and $0 \leq n \leq p$, where m, n, p and q are integer numbers
- $a_k - b_j \neq 1, 2, 3, \dots$ for $k = 1, 2, \dots, n$ and $j = 1, 2, \dots, m$
- $z \neq 0$.

Proof of Proposition 1. Derivation of Equation (4): Let $\boldsymbol{\gamma}$ be uniformly distributed on the $p - 1$ dimensional unit sphere. That is,

$$p(\boldsymbol{\gamma}) = \frac{\Gamma(p/2)}{2\pi^{p/2}} \mathbf{1} \{ \boldsymbol{\gamma}^T \boldsymbol{\gamma} = 1 \}.$$

Define $\theta = \frac{R^2}{1-R^2} \sim \text{BP}(a, b)$. Make the transformation $r = \sqrt{\theta}$:

$$\begin{aligned} p(\boldsymbol{\gamma}, \theta) &= p(\boldsymbol{\gamma})p(\theta) = \frac{\Gamma(p/2)}{2\pi^{p/2}B(a, b)} \theta^{a-1} (1 + \theta)^{-a-b} \mathbf{1} \{ \boldsymbol{\gamma}^T \boldsymbol{\gamma} = 1 \}, \\ \text{and } p(\boldsymbol{\gamma}, r) &= \frac{\Gamma(p/2)}{2\pi^{p/2}B(a, b)} r^{2a-2} (1 + r^2)^{-a-b} \mathbf{1} \{ \boldsymbol{\gamma}^T \boldsymbol{\gamma} = 1 \} |2r| \\ &= \frac{\Gamma(p/2)}{\pi^{p/2}B(a, b)} r^{2a-1} (1 + r^2)^{-a-b} \mathbf{1} \{ \boldsymbol{\gamma}^T \boldsymbol{\gamma} = 1 \}. \end{aligned}$$

Make the transformation $\mathbf{z} = r\boldsymbol{\gamma}$. The Jacobian is r^{p-1} when decomposing a vector (supported on \mathbb{R}^p) to a radius (supported in \mathbb{R}_+) and a unit direction (supported on the $p - 1$ unit sphere, \mathbb{S}_{p-1}), so the reciprocal Jacobian is $|(\mathbf{z}^T \mathbf{z})^{\frac{p-1}{2}}|^{-1} = (\mathbf{z}^T \mathbf{z})^{\frac{1-p}{2}}$. Thus,

$$\begin{aligned} p(\mathbf{z}) &= \frac{\Gamma(p/2)}{\pi^{p/2}B(a, b)} (\mathbf{z}^T \mathbf{z})^{a-1/2} (1 + \mathbf{z}^T \mathbf{z})^{-a-b} \times (\mathbf{z}^T \mathbf{z})^{\frac{1-p}{2}} \\ &= \frac{\Gamma(p/2)}{\pi^{p/2}B(a, b)} (\mathbf{z}^T \mathbf{z})^{a-p/2} (1 + \mathbf{z}^T \mathbf{z})^{-a-b} \end{aligned}$$

Finally, make the transformation $\boldsymbol{\beta} = \mathbf{V}\mathbf{D}^{-1/2}\mathbf{z}\sigma$, so that $\mathbf{z}^T\mathbf{z} = \boldsymbol{\beta}^T\mathbf{X}^T\mathbf{X}\boldsymbol{\beta}/(\sigma^2n)$, where $\mathbf{V}\mathbf{D}\mathbf{V}^T$ is the eigendecomposition of $\mathbf{X}^T\mathbf{X}/n = \boldsymbol{\Sigma}_{\mathbf{X}}$:

$$\begin{aligned} p(\boldsymbol{\beta} \mid \sigma^2) &= \frac{\Gamma(p/2)}{\pi^{p/2}B(a, b)} (\boldsymbol{\beta}^T\mathbf{X}^T\mathbf{X}\boldsymbol{\beta}/(\sigma^2n))^{a-p/2} (1 + \boldsymbol{\beta}^T\mathbf{X}^T\mathbf{X}\boldsymbol{\beta}/(\sigma^2n))^{-a-b} |\mathbf{V}\mathbf{D}^{-1/2}\sigma|^{-1} \\ &= \frac{\Gamma(p/2) |\boldsymbol{\Sigma}_{\mathbf{X}}|^{1/2}}{B(a, b) \pi^{p/2}} (\sigma^2)^{-a} (\boldsymbol{\beta}^T\boldsymbol{\Sigma}_{\mathbf{X}}\boldsymbol{\beta})^{a-p/2} (1 + \boldsymbol{\beta}^T\boldsymbol{\Sigma}_{\mathbf{X}}\boldsymbol{\beta}/\sigma^2)^{-(a+b)}. \end{aligned}$$

□

Proof of Proposition 2. Mixture of normals representation for $a \leq p/2$.

$$\text{Let } \boldsymbol{\beta} \mid z, w, \boldsymbol{\Sigma} \sim N\left(0, zw\sigma^2 (\mathbf{X}^T\mathbf{X})^{-1}\right),$$

$$z \sim \text{Inverse-Gamma}(b, n/2), \text{ and}$$

$$w \sim \text{beta}(a, p/2 - a).$$

Define $\theta = \frac{1-w}{w}$, so $\theta \sim \text{BP}(p/2 - a, a)$. To simplify notation let $\boldsymbol{\Sigma} = \mathbf{X}^T\mathbf{X}/\sigma^2$ and $\boldsymbol{\Sigma}_{\mathbf{X}} = \mathbf{X}^T\mathbf{X}/n$. Then we have

$$\begin{aligned} p(\boldsymbol{\beta}, \theta, z \mid \boldsymbol{\Sigma}) &= (2\pi)^{-p/2} z^{-p/2} (1 + \theta)^{p/2} |\boldsymbol{\Sigma}|^{1/2} \exp\left\{-\frac{1 + \theta}{2z} \boldsymbol{\beta}^T \boldsymbol{\Sigma} \boldsymbol{\beta}\right\} \\ &\quad \times \frac{n^b 2^{-b}}{\Gamma(b)} z^{-b-1} \exp\{-n/2z\} \frac{\Gamma(p/2)}{\Gamma(a)\Gamma(p/2 - a)} \theta^{p/2-a-1} (1 + \theta)^{-p/2} \\ &= \frac{2^{-p/2-b} n^b |\boldsymbol{\Sigma}|^{1/2} \Gamma(p/2)}{\pi^{p/2} \Gamma(a) \Gamma(b) \Gamma(p/2 - a)} z^{-p/2-b-1} \theta^{p/2-a-1} \exp\left\{-\frac{n + \boldsymbol{\beta}^T \boldsymbol{\Sigma} \boldsymbol{\beta} + \theta \boldsymbol{\beta}^T \boldsymbol{\Sigma} \boldsymbol{\beta}}{2z}\right\}, \end{aligned}$$

and

$$\begin{aligned} p(\boldsymbol{\beta}, z \mid \boldsymbol{\Sigma}) &= \frac{2^{-\frac{p}{2}-b} n^b |\boldsymbol{\Sigma}|^{1/2} \Gamma(\frac{p}{2})}{\pi^{\frac{p}{2}} \Gamma(a) \Gamma(b) \Gamma(\frac{p}{2} - a)} z^{-\frac{p}{2}-b-1} \exp\left\{-\frac{n + \boldsymbol{\beta}^T \boldsymbol{\Sigma} \boldsymbol{\beta}}{2z}\right\} \int \theta^{\frac{p}{2}-a-1} \exp\left\{-\theta \frac{\boldsymbol{\beta}^T \boldsymbol{\Sigma} \boldsymbol{\beta}}{2z}\right\} d\theta \\ &= \frac{2^{-a-b} n^b |\boldsymbol{\Sigma}|^{1/2} \Gamma(\frac{p}{2})}{\pi^{\frac{p}{2}} \Gamma(a) \Gamma(b)} z^{-a-b-1} \exp\left\{-\frac{n + \boldsymbol{\beta}^T \boldsymbol{\Sigma} \boldsymbol{\beta}}{2z}\right\} (\boldsymbol{\beta}^T \boldsymbol{\Sigma} \boldsymbol{\beta})^{a-\frac{p}{2}}. \end{aligned}$$

Hence then

$$\begin{aligned} p(\boldsymbol{\beta} \mid \boldsymbol{\Sigma}) &= \frac{2^{-a-b} n^b |\boldsymbol{\Sigma}|^{1/2} \Gamma(p/2)}{\pi^{p/2} \Gamma(a) \Gamma(b)} (\boldsymbol{\beta}^T \boldsymbol{\Sigma} \boldsymbol{\beta})^{a-p/2} \int z^{-a-b-1} \exp\left\{-\frac{n + \boldsymbol{\beta}^T \boldsymbol{\Sigma} \boldsymbol{\beta}}{2z}\right\} dz \\ &= \frac{2^{-a-b} n^b |\boldsymbol{\Sigma}|^{1/2} \Gamma(p/2)}{\pi^{p/2} \Gamma(a) \Gamma(b)} (\boldsymbol{\beta}^T \boldsymbol{\Sigma} \boldsymbol{\beta})^{a-p/2} (n + \boldsymbol{\beta}^T \boldsymbol{\Sigma} \boldsymbol{\beta})^{-a-b} 2^{a+b} \Gamma(a+b) \\ &= \frac{|n\boldsymbol{\Sigma}|^{1/2} \Gamma(p/2)}{\pi^{p/2} B(a, b)} (\boldsymbol{\beta}^T \boldsymbol{\Sigma} \boldsymbol{\beta}/n)^{a-p/2} (1 + \boldsymbol{\beta}^T \boldsymbol{\Sigma} \boldsymbol{\beta}/n)^{-(a+b)} \\ &= \frac{\Gamma(p/2) |\boldsymbol{\Sigma}_{\mathbf{X}}|^{1/2}}{B(a, b) \pi^{p/2}} (\sigma^2)^{-a} (\boldsymbol{\beta}^T \boldsymbol{\Sigma}_{\mathbf{X}} \boldsymbol{\beta})^{a-p/2} (1 + \boldsymbol{\beta}^T \boldsymbol{\Sigma}_{\mathbf{X}} \boldsymbol{\beta}/\sigma^2)^{-(a+b)}. \end{aligned}$$

□

Proof of Proposition 3. If we let $\mathbf{\Lambda}^{-1} = \mathbf{X}^T \mathbf{X} = n\mathbf{V}\mathbf{D}\mathbf{V}^T$, then

$$p(\boldsymbol{\gamma}) = C_{X,\Lambda} \exp \left\{ -\boldsymbol{\gamma}^T \mathbf{D}^{-1/2} \mathbf{V}^T \mathbf{V} \mathbf{D} \mathbf{V}^T \mathbf{V} \mathbf{D}^{-1/2} \boldsymbol{\gamma} / 2 \right\} \mathbb{1} \left\{ \boldsymbol{\gamma}^T \boldsymbol{\gamma} = 1 \right\} = \frac{1}{C} \mathbb{1} \left\{ \boldsymbol{\gamma}^T \boldsymbol{\gamma} = 1 \right\}$$

where the constant $C = \int \mathbb{1} \left\{ \boldsymbol{\gamma}^T \boldsymbol{\gamma} = 1 \right\} d\boldsymbol{\gamma} = \frac{2\pi^{p/2}}{\Gamma(p/2)}$, the surface area of the a $p - 1$ dimensional unit sphere. The rest of the proof is identical to that of Proposition 1 deriving the distribution in (4). It is clear that $\boldsymbol{\beta}$ is uniform given the ellipsoid, because it's an elliptical distribution, but it also comes from putting a uniform distribution on $\boldsymbol{\gamma}$. □

Proof of Proposition 4. The proposition follows from below derivations. For $\omega > 0$,

$$\begin{aligned} \pi(\omega) &= \int_0^\infty \pi(\omega | \xi) \pi(\xi) d\xi = \int_0^\infty \frac{\xi^a}{\Gamma(a)} \omega^{a-1} e^{-\xi\omega} \frac{1}{\Gamma(b)} \xi^{b-1} e^{-\xi} d\xi \\ &= \frac{1}{\Gamma(a)\Gamma(b)} \omega^{a-1} \int_0^\infty \xi^{a+b-1} e^{-(1+\omega)\xi} d\xi \\ &= \frac{1}{\Gamma(a)\Gamma(b)} \omega^{a-1} \frac{\Gamma(a+b)}{(1+\omega)^{a+b}} \\ &= \frac{\Gamma(a+b)}{\Gamma(a)\Gamma(b)} \frac{\omega^{a-1}}{(1+\omega)^{a+b}}. \end{aligned}$$

□

Proof of Proposition 5 . The proposition follows from Lemma IV.3 of Zhou & Carin (2015): Suppose y and (y_1, \dots, y_K) are independent with $y \sim \text{Ga}(\phi, \xi)$, and $(y_1, \dots, y_K) \sim \text{Dir}(\phi p_1, \dots, \phi p_K)$, where $\sum_{k=1}^K p_k = 1$. Let $x_k = y y_k$, then $x_k \sim \text{Ga}(\phi p_k, \xi)$ independently for $k = 1, \dots, K$. □

Proof of Proposition 6 . The marginal density of β for the R2-D2 prior is

$$\begin{aligned} &\pi_{\text{R2-D2}}(\beta) \\ &= \frac{\Gamma(a_\pi + b)}{\Gamma(a_\pi)\Gamma(b)} \int_0^\infty \frac{1}{2(\lambda/2)^{1/2}} \exp\left\{-\frac{|\beta|}{(\lambda/2)^{1/2}}\right\} \frac{\lambda^{a_\pi-1}}{(1+\lambda)^{a_\pi+b}} d\lambda \\ &= \frac{2^{a_\pi}\Gamma(a_\pi + b)}{\Gamma(a_\pi)\Gamma(b)} \int_0^\infty \exp(-|\beta|x) \frac{x^{2b}}{(x^2 + 2)^{a_\pi+b}} dx. \end{aligned} \tag{14}$$

Let $\mu = |\beta|$, $\nu = b + 1/2$, $u^2 = 2$, and $\rho = 1 - a_\pi - b$, since $|\arg u| < \pi/2$, $\operatorname{Re}\mu > 0$, and $\operatorname{Re}\nu > 0$, so we have

$$\begin{aligned}
\pi_{\text{R2-D2}}(\beta) &= \frac{2^{a_\pi}\Gamma(a_\pi + b)}{\Gamma(a_\pi)\Gamma(b)} \int_0^\infty \exp(-\mu x) x^{2\nu-1} (x^2 + u^2)^{\rho-1} dx \\
&= \frac{2^{a_\pi}\Gamma(a_\pi + b)}{\Gamma(a_\pi)\Gamma(b)} \frac{u^{2\nu+2\rho-2}}{2\pi^{1/2}\Gamma(1-\rho)} G_{1,3}^{3,1} \left(\frac{\mu^2 u^2}{4} \left| \begin{matrix} 1-\nu \\ 1-\rho-\nu, 0, \frac{1}{2} \end{matrix} \right. \right) \\
&= \frac{2^{a_\pi}\Gamma(a_\pi + b)}{\Gamma(a_\pi)\Gamma(b)} \frac{2^{1/2-a_\pi}}{2\pi^{1/2}\Gamma(a_\pi + b)} G_{1,3}^{3,1} \left(\frac{\beta^2}{2} \left| \begin{matrix} \frac{1}{2}-b \\ a_\pi-\frac{1}{2}, 0, \frac{1}{2} \end{matrix} \right. \right) \\
&= \frac{1}{(2\pi)^{1/2}\Gamma(a_\pi)\Gamma(b)} G_{1,3}^{3,1} \left(\frac{\beta^2}{2} \left| \begin{matrix} \frac{1}{2}-b \\ a_\pi-\frac{1}{2}, 0, \frac{1}{2} \end{matrix} \right. \right) \\
&= \frac{1}{(2\pi)^{1/2}\Gamma(a_\pi)\Gamma(b)} G_{3,1}^{1,3} \left(\frac{2}{\beta^2} \left| \begin{matrix} \frac{3}{2}-a_\pi, 1, \frac{1}{2} \\ \frac{1}{2}+b \end{matrix} \right. \right)
\end{aligned}$$

where $G(\cdot)$ denotes the Meijer G-Function, the second equality follows from equation 3.389.2 in Zwillinger (2014), and the last equality follows from 16.19.1 in DLMF (2015). Proposition 6 follows. \square

Proof of Theorem 1. For the proof of Theorem 1, we will use the following lemma found in Miller (2006).

Lemma 1. (*Watson's Lemma*) Suppose $F(s) = \int_0^\infty e^{-st} f(t) dt$, $f(t) = t^\alpha g(t)$ where $g(t)$ has an infinite number of derivatives in the neighborhood of $t = 0$, with $g(0) \neq 0$, and $\alpha > -1$. Suppose $|f(t)| < Ke^{ct}$ for any $t \in (0, \infty)$, where K and c are independent of t . Then, for $s > 0$ and $s \rightarrow \infty$,

$$F(s) = \sum_{k=0}^n \frac{g^{(k)}(0)}{k!} \frac{\Gamma(\alpha + k + 1)}{s^{\alpha+k+1}} + O\left(\frac{1}{s^{\alpha+n+2}}\right).$$

According to equation (14) in the proof of Proposition 6, we denote $F(|\beta|) \equiv \pi_{\text{R2-D2}}(\beta)$, as follows,

$$F(|\beta|) = \frac{2^{a_\pi}\Gamma(a_\pi + b)}{\Gamma(a_\pi)\Gamma(b)} \int_0^\infty \exp(-|\beta|x) \frac{x^{2b}}{(x^2 + 2)^{a_\pi+b}} dx = \int_0^\infty e^{-|\beta|x} f(x) dx,$$

where $f(t) = C^* t^{2b} / (t^2 + 2)^{a_\pi+b} \equiv t^{2b} g(t)$, $C^* = 2^{a_\pi}\Gamma(a_\pi + b) / \{\Gamma(a_\pi)\Gamma(b)\}$, and $g(t) = C^*(t^2 + 2)^{-a_\pi-b}$ with $g(t)$ has an infinite number of derivatives in the neighborhood of $t = 0$, with $g(0) \neq 0$. So the marginal density of R2-D2 prior is the Laplace transforms

of $f(\cdot)$. By Watson's Lemma, since $|f(t)| < Ke^{ct}$ for any $t \in (0, \infty)$, where K and c are independent of t , then as $|\beta| \rightarrow \infty$,

$$F(|\beta|) = \sum_{k=0}^n \frac{g^{(k)}(0)}{k!} \frac{\Gamma(2b+k+1)}{|\beta|^{2b+k+1}} + O\left(\frac{1}{|\beta|^{2b+n+2}}\right),$$

and setting $n = 2$ gives

$$\begin{aligned} F(|\beta|) &= C^* \left\{ \frac{\Gamma(2b+1)}{2^{a_\pi+b}|\beta|^{2b+1}} + 0 \frac{\Gamma(2b+2)}{|\beta|^{2b+2}} - \frac{a_\pi+b}{2^{a_\pi+b}|\beta|^{2b+3}} \Gamma(2b+3) \right\} + O\left(\frac{1}{|\beta|^{2b+4}}\right) \\ &= C^* 2^{-a_\pi-b} \left\{ \frac{\Gamma(2b+1)}{|\beta|^{2b+1}} - (a_\pi+b) \frac{\Gamma(2b+3)}{|\beta|^{2b+3}} \right\} + O\left(\frac{1}{|\beta|^{2b+4}}\right) \\ &= O\left(\frac{1}{|\beta|^{2b+1}}\right). \end{aligned} \tag{15}$$

Hence, when $b < 1/2$, as $|\beta| \rightarrow \infty$, we have

$$\frac{\pi_{R2-D2}(\beta)}{\frac{1}{\beta^2}} = \frac{C^*}{2^{a_\pi+b}} \left\{ \frac{\Gamma(2b+1)}{|\beta|^{2b-1}} - (a_\pi+b) \frac{\Gamma(2b+3)}{|\beta|^{2b+1}} + O\left(\frac{1}{|\beta|^{2b+2}}\right) \right\} \rightarrow \infty.$$

□

Proof of Theorem 2. It is obvious based on the marginal density of the generalized double Pareto prior. □

Proof of Theorem 3. According to 10.25.3 in DLMF (2015), when both ν and z are real, if $z \rightarrow \infty$, then $K_\nu(z) \approx \pi^{1/2}(2z)^{-1/2}e^{-z}$. Then as $|\beta| \rightarrow \infty$, the marginal density of the Dirichlet-Laplace prior given in Bhattacharya et al. (2015) satisfies

$$\begin{aligned} \pi_{DL}(\beta) &= \frac{1}{2^{(1+a^*)/2}\Gamma(a^*)} |\beta|^{(a^*-1)/2} K_{1-a^*}((2|\beta|)^{1/2}) \\ &\approx \frac{1}{2^{(1+a^*)/2}\Gamma(a^*)} |\beta|^{(a^*-1)/2} \pi^{1/2} 2^{-3/4} |\beta|^{-1/4} \exp\{-\sqrt{2|\beta|}\} \\ &= C_0 |\beta|^{a^*/2-3/4} \exp\{-\sqrt{2|\beta|}\} = O\left(\frac{|\beta|^{a^*/2-3/4}}{\exp\{\sqrt{2|\beta|}\}}\right), \end{aligned}$$

where $C_0 = \pi^{1/2} 2^{-3/4} / \{2^{(1+a^*)/2} \Gamma(a^*)\}$ is a constant value. Furthermore, as $|\beta| \rightarrow \infty$,

$$\frac{\pi_{DL}(\beta)}{1/\beta^2} \approx C_0 |\beta|^{a^*/2+5/4} \exp\{-\sqrt{2|\beta|}\} \rightarrow 0.$$

□

Proof of Theorem 4. For the proof of Theorem 4, we use the following lemma from Fields (1972). Some useful notations used in the below proof: Denote $a_P = (a_1, \dots, a_p)$, as a vector, similarly, $b_Q = (b_1, \dots, b_q)$, $c_M = (c_1, \dots, c_m)$, and so on. Let $\Gamma_n(c_P - t) = \prod_{k=n+1}^p \Gamma(c_k - t)$, with $\Gamma_n(c_P - t) = 1$ when $n = p$, $\Gamma(c_M - t) = \Gamma_0(c_M - t) = \prod_{k=1}^m \Gamma(c_k - t)$, $\Gamma^*(a_i - a_N) = \prod_{k=1; k \neq i}^n \Gamma(a_i - a_k)$, and

$${}_pF_q \left(\begin{matrix} a_P \\ b_Q \end{matrix} \middle| w \right) = \sum_{k=0}^{\infty} \frac{\Gamma(a_P + k) \Gamma(b_Q) w^k}{\Gamma(b_Q + k) \Gamma(a_P) k!} = \sum_{k=0}^{\infty} \frac{\prod_{j=1}^p \Gamma(a_j + k) \prod_{j=1}^q \Gamma(b_j)}{\prod_{j=1}^q \Gamma(b_j + k) \prod_{j=1}^p \Gamma(a_j)} \frac{w^k}{k!}.$$

Lemma 2. (Theorem 1 in Fields (1972)) Given (i) $0 \leq m \leq q$, $0 \leq n \leq p$; (ii) $a_i - b_k$ is not a positive integer for $j = 1, \dots, p$ and $k = 1, \dots, q$; (iii) $a_i - a_k$ is not an integer for $i, k = 1, \dots, p$, and $i \neq k$; and (iv) $q < p$ or $q = p$ and $|z| > 1$, we have

$$G_{p,q}^{m,n} \left(z \middle| \begin{matrix} a_1, \dots, a_p \\ b_1, \dots, b_q \end{matrix} \right) = \sum_{i=1}^n \frac{\Gamma^*(a_i - a_N) \Gamma(1 + b_M - a_i) z^{-1+a_i}}{\Gamma_n(1 + a_P - a_i) \Gamma_m(a_i - b_Q)} {}_{q+1}F_p \left(\begin{matrix} 1, 1+b_Q-a_i \\ 1+a_P-a_i \end{matrix} \middle| \frac{(-1)^{q-m-n}}{z} \right).$$

Now to prove Theorem 4, we have from Proposition 6 that, the marginal density of the R2-D2 prior has $\pi_{\text{R2-D2}}(\beta_j) = (2\pi)^{-1/2} \{\Gamma(a_\pi) \Gamma(b)\}^{-1} G_{p,q}^{m,n}(z|\cdot)$ with $m = 1$, $n = 3$, $p = 3$, $q = 1$, $a_1 = 3/2 - a_\pi$, $a_2 = 1$, $a_3 = 1/2$, $b_1 = 1/2 + b$, and $z = 2/\beta^2$. Conditions (i)-(iv) in Lemma 2 are satisfied for $|\beta|$ near 0, since $0 < a_\pi < 1/2$. Denote

$$\begin{aligned} C_0^* &= (2\pi)^{-1/2} (\Gamma(a_\pi) \Gamma(b))^{-1}, \\ C_1^* &= C_0^* \Gamma\left(\frac{1}{2} - a_\pi\right) \Gamma(1 - a_\pi) \Gamma(a_\pi) \Gamma\left(\frac{1}{2} + a_\pi\right) > 0, \\ C_2^* &= C_0^* \Gamma\left(a_\pi - \frac{1}{2}\right) \Gamma\left(\frac{1}{2}\right) \Gamma\left(\frac{1}{2}\right) \Gamma\left(\frac{3}{2} - a_\pi\right) < 0, \\ C_3^* &= C_0^* \Gamma(a_\pi - 1) \Gamma\left(-\frac{1}{2}\right) \Gamma\left(\frac{3}{2}\right) \Gamma(2 - a_\pi) > 0, \\ U_1(\beta^2) &= \sum_{k=0}^{\infty} (-1)^k u_1(k, \beta^2), \quad u_1(k, \beta^2) = \frac{\Gamma(a_\pi + b + k)}{\Gamma\left(\frac{1}{2} + a_\pi + k\right) \Gamma(a_\pi + k)} \frac{\left(\frac{\beta^2}{2}\right)^{k+a_\pi-1/2}}{k!}, \\ U_2(\beta^2) &= \sum_{k=0}^{\infty} (-1)^k u_2(k, \beta^2), \quad u_2(k, \beta^2) = \frac{\Gamma\left(\frac{1}{2} + b + k\right)}{\Gamma\left(\frac{3}{2} - a_\pi + k\right) \Gamma\left(\frac{1}{2} + k\right)} \frac{\left(\frac{\beta^2}{2}\right)^k}{k!}, \\ \text{and } U_3(\beta^2) &= \sum_{k=0}^{\infty} (-1)^k u_3(k, \beta^2), \quad u_3(k, \beta^2) = \frac{\Gamma(1 + b + k)}{\Gamma(2 - a_\pi + k) \Gamma\left(\frac{3}{2} + k\right)} \frac{\left(\frac{\beta^2}{2}\right)^{k+1/2}}{k!}. \end{aligned}$$

Then

$$\begin{aligned}
\pi_{\text{R2-D2}}(\beta) &= C_0^* G_{3,1}^{1,3} \left(\frac{2}{\beta^2} \middle| \frac{\frac{3}{2} - a_\pi, 1, \frac{1}{2}}{\frac{1}{2} + b} \right) \\
&= C_0^* \sum_{i=1}^3 \frac{\Gamma^*(a_i - a_N) \Gamma(1 + b_M - a_i)}{\Gamma_3(1 + a_P - a_i) \Gamma_1(a_i - b_Q)} \left(\frac{2}{\beta^2} \right)^{-1+a_i} {}_2F_3 \left(\begin{matrix} 1, 1+b_Q-a_i \\ 1+a_P-a_i \end{matrix} \middle| \frac{-\beta^2}{2} \right) \\
&= C_0^* \sum_{i=1}^3 \frac{\prod_{k=1; k \neq i}^3 \Gamma(a_i - a_k) \Gamma(1 + b_1 - a_i)}{\prod_{k=3+1}^3 \Gamma(1 + a_k - a_i) \prod_{k=1+1}^1 \Gamma(a_i - b_k)} \left(\frac{2}{\beta^2} \right)^{-1+a_i} {}_2F_3 \left(\begin{matrix} 1, 1+b_1-a_i \\ 1+a_P-a_i \end{matrix} \middle| \frac{-\beta^2}{2} \right) \\
&= C_0^* \sum_{i=1}^3 \left\{ \frac{\prod_{k=1; k \neq i}^3 \Gamma(a_i - a_k) \Gamma(1 + b_1 - a_i)}{1} \left(\frac{2}{\beta^2} \right)^{-1+a_i} \times \right. \\
&\quad \left. \sum_{k=0}^{\infty} \frac{\Gamma(1+k) \Gamma(1+b_1-a_i+k) \prod_{j=1}^3 \Gamma(1+a_j-a_i)}{\prod_{j=1}^3 \Gamma(1+a_j-a_i+k) \Gamma(1) \Gamma(1+b_1-a_i)} \frac{\left(\frac{-\beta^2}{2} \right)^k}{k!} \right\} \\
&= C_0^* \times \\
&\quad \left\{ \Gamma\left(\frac{1}{2} - a_\pi\right) \Gamma(1 - a_\pi) \sum_{k=0}^{\infty} \frac{\Gamma(a_\pi + b + k) \Gamma\left(\frac{1}{2} + a_\pi\right) \Gamma(a_\pi)}{\Gamma\left(\frac{1}{2} + a_\pi + k\right) \Gamma(a_\pi + k)} \frac{(-1)^k \left(\frac{\beta^2}{2}\right)^{k+a_\pi-1/2}}{k!} \right. \\
&\quad + \Gamma\left(a_\pi - \frac{1}{2}\right) \Gamma\left(\frac{1}{2}\right) \Gamma\left(\frac{1}{2}\right) \sum_{k=0}^{\infty} \frac{\Gamma\left(\frac{1}{2} + b + k\right) \Gamma\left(\frac{3}{2} - a_\pi\right)}{\Gamma\left(\frac{3}{2} - a_\pi + k\right) \Gamma\left(\frac{1}{2} + k\right)} \frac{(-1)^k \left(\frac{\beta^2}{2}\right)^k}{k!} \\
&\quad \left. + \Gamma(a_\pi - 1) \Gamma\left(-\frac{1}{2}\right) \Gamma\left(\frac{3}{2}\right) \sum_{k=0}^{\infty} \frac{\Gamma(1+b+k) \Gamma(2-a_\pi)}{\Gamma(2-a_\pi+k) \Gamma\left(\frac{3}{2} + k\right)} \frac{(-1)^k \left(\frac{\beta^2}{2}\right)^{k+1/2}}{k!} \right\} \\
&\equiv C_0^* \times \left\{ \Gamma\left(\frac{1}{2} - a_\pi\right) \Gamma(1 - a_\pi) \Gamma(a_\pi) \Gamma\left(\frac{1}{2} + a_\pi\right) U_1(\beta^2) + \right. \\
&\quad \left. \Gamma\left(a_\pi - \frac{1}{2}\right) \Gamma\left(\frac{1}{2}\right) \Gamma\left(\frac{1}{2}\right) \Gamma\left(\frac{3}{2} - a_\pi\right) U_2(\beta^2) + \Gamma(a_\pi - 1) \Gamma\left(-\frac{1}{2}\right) \Gamma\left(\frac{3}{2}\right) \Gamma(2 - a_\pi) U_3(\beta^2) \right\} \\
&\equiv C_1^* U_1(\beta^2) + C_2^* U_2(\beta^2) + C_3^* U_3(\beta^2).
\end{aligned}$$

For fixed β near the neighborhood of zero, $u_1(k, \beta^2)$, $u_2(k, \beta^2)$, and $u_3(k, \beta^2)$ are all monotone decreasing, and converge to zero as $k \rightarrow \infty$. Thus, by alternating series test, $U_1(\beta^2)$, $U_2(\beta^2)$, and $U_3(\beta^2)$ all converge. Also, we have

$$C_0 |\beta|^{2a_\pi-1} - C_1 |\beta|^{2a_\pi+1} = u_1(0, \beta^2) - u_1(1, \beta^2) \leq U_1(\beta^2) \leq u_1(0, \beta^2) = C_0 |\beta|^{2a_\pi-1}$$

$$C_2 - C_3|\beta|^2 = u_2(0, \beta^2) - u_2(1, \beta^2) \leq U_2(\beta^2) \leq u_2(0, \beta^2) = C_2$$

$$C_4|\beta| - C_5|\beta|^3 = u_3(0, \beta^2) - u_3(1, \beta^2) \leq U_3(\beta^2) \leq u_3(0, \beta^2) = C_4|\beta|$$

where $C_0, C_1, C_2, C_3,$ and C_4 are all positive constants. So given that $|\beta|$ in the neighborhood of zero and $a_\pi \in (0, \frac{1}{2})$, $C_1^*(C_0|\beta|^{2a_\pi-1} - C_1|\beta|^{2a_\pi+1}) + C_2^*C_2 + C_3^*(C_4|\beta| - C_5|\beta|^3) \leq \pi_{\text{R2-D2}}(\beta) \leq C_1^*C_0|\beta|^{2a_\pi-1} + C_2^*(C_2 - C_3|\beta|^2) + C_3^*C_4|\beta|$, then $\pi_{\text{R2-D2}}(\beta) = O(|\beta|^{2a_\pi-1})$. \square

Proof of Theorem 5. According to 10.30.2 in DLMF (2015), when $\nu > 0$, $z \rightarrow 0$ and z is real, $K_\nu(z) \approx \Gamma(\nu)(z/2)^{-\nu}/2$. So given $0 < a^* < 1$ and $|\beta| \rightarrow 0$,

$$\begin{aligned} \pi_{\text{DL}}(\beta) &= \frac{|\beta|^{(a^*-1)/2} K_{1-a^*}((2|\beta|)^{1/2})}{2^{(1+a^*)/2} \Gamma(a^*)} \\ &\approx \frac{|\beta|^{(a^*-1)/2} \frac{1}{2} \Gamma(1-a^*) \left(\frac{(2|\beta|)^{1/2}}{2}\right)^{a^*-1}}{2^{(1+a^*)/2} \Gamma(a^*)} = C|\beta|^{a^*-1}, \end{aligned}$$

where $C = \Gamma(1-a^*)/2^{1+a^*} \Gamma(a^*)$ is a constant value. Theorem 5 follows then. \square

Proof of Theorem 6. The proof of this theorem depends on Theorem 1 in Armagan, Dunson, Lee, Bajwa & Strawn (2013). We will restate this theorem in the following Lemma.

Lemma 3. *Under Assumptions (A1) and (A2), the posterior of β_n under prior $\pi_n(\beta_n)$ is strongly consistent, that is, for any $\epsilon > 0$, as $n \rightarrow \infty$,*

$$Pr_{\beta_n^0} \left\{ \pi_n(\beta_n : \|\beta_n - \beta_n^0\| > \epsilon \mid Y_n) \rightarrow 0 \right\} = 1$$

if

$$\pi_n(\beta_n : \|\beta_n - \beta_n^0\| < \frac{\Delta}{n^{r/2}}) > \exp(-dn)$$

for all $0 < \Delta < \epsilon^2 d_{\min}/(48d_{\max})$ and $0 < d < \epsilon^2 d_{\min}/(32\sigma^2) - 3\Delta d_{\max}/(2\sigma^2)$ and some $r > 0$.

Denote the estimated set of non-zero coefficients as $\mathcal{A}_n = \{j : \beta_{nj} \neq 0, j = 1, \dots, p_n\}$. Given the R2-D2 prior (9), we need to calculate the probability assigned to the region $\{\beta : \|\beta - \beta^0\| < t_n\}$ where $t_n = \Delta/n^{r/2}$ with $0 < \Delta < \epsilon^2 d_{\min}/(48d_{\max})$.

$$\begin{aligned}
& \pi_n(\boldsymbol{\beta}_n : \|\boldsymbol{\beta}_n - \boldsymbol{\beta}_n^0\| < t_n) = \pi_n \left\{ \boldsymbol{\beta}_n : \sum_{j \in \mathcal{A}_n} (\beta_{nj} - \beta_{nj}^0)^2 + \sum_{j \notin \mathcal{A}_n} \beta_{nj}^2 < t_n^2 \right\} \\
& \geq \pi_n \left\{ \boldsymbol{\beta}_{n_j}^{j \in \mathcal{A}_n} : \sum_{j \in \mathcal{A}_n} (\beta_{nj} - \beta_{nj}^0)^2 < \frac{q_n t_n^2}{p_n} \right\} \times \pi_n \left\{ \boldsymbol{\beta}_{n_j}^{j \notin \mathcal{A}_n} : \sum_{j \notin \mathcal{A}_n} \beta_{nj}^2 < \frac{(p_n - q_n) t_n^2}{p_n} \right\} \\
& \geq \left[\prod_{j \in \mathcal{A}_n} \left\{ \pi_n \left(\beta_{nj} : |\beta_{nj} - \beta_{nj}^0| < \frac{t_n}{\sqrt{p_n}} \right) \right\} \right] \pi_n \left(\boldsymbol{\beta}_{n_j}^{j \notin \mathcal{A}_n} : \beta_{nj}^2 < \frac{t_n^2}{p_n} \text{ at least for one } j \right) \\
& = \left[\prod_{j \in \mathcal{A}_n} \left\{ \pi_n \left(\beta_{nj}^0 - \frac{t_n}{\sqrt{p_n}} < \beta_{nj} < \beta_{nj}^0 + \frac{t_n}{\sqrt{p_n}} \right) \right\} \right] \left[1 - \left\{ \pi_n \left(\boldsymbol{\beta}_{n_j}^{j \notin \mathcal{A}_n} : \beta_{nj}^2 \geq \frac{t_n^2}{p_n} \right) \right\}^{p_n - q_n} \right] \\
& \geq \left\{ \prod_{j \in \mathcal{A}_n} 2 \frac{t_n}{\sqrt{p_n}} \pi_{\text{R2-D2}} \left(|\beta_{nj}^0| + \frac{t_n}{\sqrt{p_n}} \right) \right\} \left[1 - \left\{ \pi_n \left(\boldsymbol{\beta}_{n_j}^{j \notin \mathcal{A}_n} : |\beta_{nj}|^b \geq \frac{t_n^b}{p_n^{b/2}} \right) \right\}^{p_n - q_n} \right] \\
& \geq \left\{ \prod_{j \in \mathcal{A}_n} 2 \frac{t_n}{\sqrt{p_n}} \pi_{\text{R2-D2}} \left(\sup_{j \in \mathcal{A}_n} |\beta_{nj}^0| + \frac{t_n}{\sqrt{p_n}} \right) \right\} \left[1 - \left\{ \frac{p_n^{b/2} \mathbf{E}(|\beta_{nj}|^b)}{t_n^b} \right\}^{p_n - q_n} \right] \\
& \geq \left\{ 2 \frac{t_n}{\sqrt{p_n}} \pi_{\text{R2-D2}} \left(\sup_{j \in \mathcal{A}_n} |\beta_{nj}^0| + \frac{t_n}{\sqrt{p_n}} \right) \right\}^{q_n} \times \left[1 - \left\{ \frac{p_n^{b/2} \mathbf{E}(|\beta_{nj}|^b)}{t_n^b} \right\}^{p_n - q_n} \right],
\end{aligned}$$

where $\pi_{\text{R2-D2}}(\cdot)$ is the marginal density function of β_{nj} , symmetric and decreasing when the support is positive, and the last but one “ \geq ” is directly got from Markov’s inequality.

Using the hierarchical form of the R2-D2 prior in (10), for any $b > 0$, conditional expectations yield

$$\mathbf{E}(|\beta_{nj}|^b) = \mathbf{E}[\mathbf{E}\{\mathbf{E}(|\beta_{nj}|^b \mid \lambda_j) \mid \xi\}] = \mathbf{E}_\xi \left[\mathbf{E}_{\lambda_j \mid \xi} \left\{ \frac{\Gamma(b+1)}{(2/\lambda_j)^{b/2}} \mid \xi \right\} \right] = \frac{b\Gamma(\frac{b}{2})\Gamma(a_\pi + \frac{b}{2})}{2^{b/2}\Gamma(a_\pi)}.$$

For the R2-D2 prior, from equation (14), it follows that the marginal density is a decreasing function on the positive support. Then assumptions (A1) – (A4), together with the tail approximation of the marginal density as in the proof of Theorem 1, i.e., equation (15), we have

$$\pi_{\text{R2-D2}} \left(\sup_{j \in \mathcal{A}_n} |\beta_{nj}^0| + \frac{t_n}{\sqrt{p_n}} \right) \geq \pi_{\text{R2-D2}} \left(E_n + \frac{t_n}{\sqrt{p_n}} \right) \geq \frac{\Gamma(a_\pi + b)}{\Gamma(a_\pi)\Gamma(b)} 2^{-b} \frac{\Gamma(2b+1)}{\left(E_n + \frac{\Delta}{nr^{1/2}\sqrt{p_n}} \right)^{2b+1}}.$$

Considering the fact that $\Gamma(a) = a^{-1} - \gamma_0 + O(a)$ for a being near zero with γ_0 the

Euler-Mascheroni constant, we have

$$\begin{aligned}
& \pi_n(\boldsymbol{\beta}_n : \|\boldsymbol{\beta}_n - \boldsymbol{\beta}_n^0\| < \frac{\Delta}{n^{r/2}}) \\
& \geq \left\{ 2 \frac{\Delta}{n^{r/2} \sqrt{p_n}} \frac{\Gamma(a_\pi + b)}{\Gamma(a_\pi) \Gamma(b)} 2^{-b} \frac{\Gamma(2b + 1)}{(E_n + \frac{\Delta}{n^{r/2} \sqrt{p_n}})^{2b+1}} \right\}^{q_n} \left[1 - \left\{ \frac{p_n^{b/2} n^{rb/2} b \Gamma(\frac{b}{2}) \Gamma(a_\pi + \frac{b}{2})}{\Delta^b 2^{b/2} \Gamma(a_\pi)} \right\}^{p_n - q_n} \right] \\
& \geq \left\{ \frac{2\Delta}{n^{r/2} \sqrt{p_n}} \frac{\Gamma(a_\pi + b) a_\pi}{\Gamma(b)} 2^{-b} \frac{\Gamma(2b + 1)}{(E_n + \frac{\Delta}{n^{r/2} \sqrt{p_n}})^{2b+1}} \right\}^{q_n} \left[1 - \left\{ \frac{p_n^{b/2} n^{rb/2} b \Gamma(\frac{b}{2}) \Gamma(a_\pi + \frac{b}{2}) a_\pi}{\Delta^b 2^{b/2}} \right\}^{p_n - q_n} \right].
\end{aligned}$$

Taking the negative logarithm of both sides of the above formula, and letting $a_\pi = C/(p_n^{b/2} n^{rb/2} \log n)$, we have

$$\begin{aligned}
& -\log \pi_n(\boldsymbol{\beta}_n : \|\boldsymbol{\beta}_n - \boldsymbol{\beta}_n^0\| < \frac{\Delta}{n^{r/2}}) \\
& \leq -q_n \log \left\{ \frac{2\Delta C \Gamma(a_\pi + b) 2^{-b} \Gamma(2b + 1)}{n^{r/2} \sqrt{p_n} p_n^{b/2} n^{rb/2} \log n \Gamma(b)} \right\} + q_n (2b + 1) \log \left(E_n + \frac{\Delta}{n^{r/2} \sqrt{p_n}} \right) \\
& \quad - q_n \log \left[1 - \left\{ \frac{p_n^{b/2} n^{rb/2} b \Gamma(\frac{b}{2}) \Gamma(a_\pi + \frac{b}{2}) C}{\Delta^b 2^{b/2} p_n^{b/2} n^{rb/2} \log n} \right\}^{p_n - q_n} \right] \\
& = -q_n \log \left\{ \frac{2\Delta C \Gamma(a_\pi + b) 2^{-b} \Gamma(2b + 1)}{\Gamma(b)} \right\} + q_n (2b + 1) \log \left(E_n + \frac{\Delta}{n^{r/2} \sqrt{p_n}} \right) \\
& \quad - q_n \log \left[1 - \left\{ \frac{b \Gamma(\frac{b}{2}) \Gamma(a_\pi + \frac{b}{2}) C}{\Delta^b 2^{b/2} \log n} \right\}^{p_n - q_n} \right] + q_n \log \log n \\
& \quad + \frac{b + 1}{2} q_n \log p_n + \frac{b + 1}{2} q_n r \log n
\end{aligned}$$

Since $\log E_n = O(\log n)$, the dominating term is $O(q_n \log n)$. Hence, if $q_n = o(n/\log n)$, then we have that $-\log \pi_n(\boldsymbol{\beta}_n : \|\boldsymbol{\beta}_n - \boldsymbol{\beta}_n^0\| < \Delta/n^{r/2}) < dn$ for all $0 < d < \epsilon^2 d_{\min}/(32\sigma^2) - 3\Delta d_{\max}/(2\sigma^2)$, so $\pi_n(\boldsymbol{\beta}_n : \|\boldsymbol{\beta}_n - \boldsymbol{\beta}_n^0\| < \Delta/n^{r/2}) > \exp(-dn)$. The posterior consistency is then completed by applying Lemma 3. \square

Proof of Theorem 7. Now that we have established the properties of marginal prior for the R2-D2 hierarchical formulation, the proof will now be based on the results similar to Theorems 2.1, 2.2, A.1 and A.2 in Song & Liang (2017). We will restate these theorems in the following lemma.

Lemma 4. Consider the linear regression model (1) and suppose the regularity conditions (B2)-(B5) hold. Suppose that the prior for $\pi(\beta, \sigma^2)$ is of the form

$$\pi(\beta \mid \sigma^2) = \prod_{i=1}^p [g(\beta_i/\sigma)/\sigma], \quad \sigma^2 \sim IG(a_1, b_1).$$

Denote $\epsilon_n = M\sqrt{q_n(\log p_n)/n}$ where $M > 0$ is sufficiently large. If the density $g(\cdot)$ in the above formula satisfies

$$1 - \int_{-k_n}^{k_n} g(\beta) d\beta \leq p_n^{-(1+u)}, \quad -\log \left(\inf_{\beta \in [-E_n, E_n]} g(\beta) \right) = O(\log p_n), \quad (16)$$

where $u > 0$ is a constant and $k_n \asymp \sqrt{q_n(\log p_n)/n}/p_n$, then the following results hold:

$$Pr_{\beta^0} \left\{ \pi(\beta_n : \|\beta_n - \beta_n^0\| \geq c_1 \sigma^0 \epsilon_n \mid \mathbf{Y}_n) \geq e^{-c_2 n \epsilon_n^2} \right\} \leq e^{-c_3 n \epsilon_n^2},$$

$$Pr_{\beta^0} \left\{ \pi(\beta_n : \|\beta_n - \beta_n^0\|_1 \geq c_1 \sigma^0 \sqrt{q_n} \epsilon_n \mid \mathbf{Y}_n) \geq e^{-c_2 n \epsilon_n^2} \right\} \leq e^{-c_3 n \epsilon_n^2},$$

$$Pr_{\beta^0} \left\{ \pi(\beta_n : \|\mathbf{X}_n \beta_n - \mathbf{X}_n \beta_n^0\| \geq c_1 \sigma^0 \sqrt{n} \epsilon_n \mid \mathbf{Y}_n) \geq e^{-c_2 n \epsilon_n^2} \right\} \leq e^{-c_3 n \epsilon_n^2},$$

for some constants $c_1, c_2, c_3 > 0$.

For the R2-D2 prior in (9), according to (14) the corresponding $g(\cdot)$ function is

$$g(\beta) = \frac{2^{a_\pi} \Gamma(a_\pi + b)}{\Gamma(a_\pi) \Gamma(b)} \int_0^\infty \exp(-|\beta|x) \frac{x^{2b}}{(x^2 + 2)^{a_\pi + b}} dx.$$

By the symmetry of $g(\beta)$ and Fubini's Theorem, we have

$$\begin{aligned} 1 - \int_{-k_n}^{k_n} g(\beta) d\beta &= 2 \int_{k_n}^\infty g(\beta) d\beta \\ &= 2 \frac{2^{a_\pi} \Gamma(a_\pi + b)}{\Gamma(a_\pi) \Gamma(b)} \int_0^\infty \int_{k_n}^\infty \exp(-|\beta|x) d\beta \frac{x^{2b}}{(x^2 + 2)^{a_\pi + b}} dx \\ &= 2 \frac{2^{a_\pi} \Gamma(a_\pi + b)}{\Gamma(a_\pi) \Gamma(b)} \int_0^\infty \frac{\exp(-k_n x)}{x} \frac{x^{2b}}{(x^2 + 2)^{a_\pi + b}} dx \\ &= \frac{2\Gamma(a_\pi + b)}{\Gamma(a_\pi) \Gamma(b)} \int_0^\infty \exp(-k_n \sqrt{2}x) \frac{x^{2b-1}}{(x^2 + 1)^{a_\pi + b}} dx \\ &= \frac{2\Gamma(a_\pi + b)}{\Gamma(a_\pi) \Gamma(b)} \frac{1}{2\sqrt{\pi}\Gamma(a_\pi + b)} G_{1,3}^{3,1} \left(\frac{k_n^2}{2} \middle| \begin{matrix} 1-b \\ a_\pi, 0, \frac{1}{2} \end{matrix} \right) \\ &= \frac{1}{\sqrt{\pi}\Gamma(a_\pi) \Gamma(b)} G_{1,3}^{3,1} \left(\frac{k_n^2}{2} \middle| \begin{matrix} 1-b \\ a_\pi, 0, \frac{1}{2} \end{matrix} \right) \end{aligned}$$

where the second to last “=” follows from equation 3.389.2 in Zwillinger (2014). The right side of the above equation looks similar to the marginal density of R2-D2 prior, so we can apply exactly the same technique used in proof of Theorem 4. So in the proof

$$1 - \int_{-k_n}^{k_n} g(\beta) d\beta = \frac{1}{\sqrt{\pi}\Gamma(a_\pi)\Gamma(b)} G_{1,3}^{3,1} \left(\frac{k_n^2}{2} \middle|_{a_\pi, 0, \frac{1}{2}}^{1-b} \right) = C_1^* U_1(k_n^2) + C_2^* U_2(k_n^2) + C_3^* U_3(k_n^2),$$

where

$$\begin{aligned} C_1^* &= \frac{1}{\sqrt{\pi}\Gamma(a_\pi)\Gamma(b)} \Gamma(-a_\pi)\Gamma\left(\frac{1}{2} - a_\pi\right)\Gamma(a_\pi + \frac{1}{2})\Gamma(1 + a_\pi) < 0, \\ C_2^* &= \frac{1}{\sqrt{\pi}\Gamma(a_\pi)\Gamma(b)} \Gamma(a_\pi)\Gamma\left(\frac{1}{2}\right)\Gamma\left(\frac{1}{2}\right)\Gamma(1 - a_\pi) > 0, \\ C_3^* &= \frac{1}{\sqrt{\pi}\Gamma(a_\pi)\Gamma(b)} \Gamma(a_\pi - \frac{1}{2})\Gamma\left(-\frac{1}{2}\right)\Gamma\left(\frac{3}{2}\right)\Gamma\left(\frac{3}{2} - a_\pi\right) > 0, \\ U_1(k_n^2) &= \sum_{j=0}^{\infty} (-1)^j u_1(j, k_n^2), \quad u_1(j, k_n^2) = \frac{\Gamma(a_\pi + b + j)}{\Gamma(1 + a_\pi + j)\Gamma\left(\frac{1}{2} + a_\pi + j\right)} \frac{\left(\frac{k_n^2}{2}\right)^{j+a_\pi}}{j!}, \\ U_2(k_n^2) &= \sum_{j=0}^{\infty} (-1)^j u_2(j, k_n^2), \quad u_2(j, k_n^2) = \frac{\Gamma(b + j)}{\Gamma(1 - a_\pi + j)\Gamma\left(\frac{1}{2} + j\right)} \frac{\left(\frac{k_n^2}{2}\right)^j}{j!}, \\ \text{and } U_3(k_n^2) &= \sum_{j=0}^{\infty} (-1)^j u_3(j, k_n^2), \quad u_3(j, k_n^2) = \frac{\Gamma\left(\frac{1}{2} + b + j\right)}{\Gamma\left(\frac{3}{2} - a_\pi + j\right)\Gamma\left(\frac{3}{2} + j\right)} \frac{\left(\frac{k_n^2}{2}\right)^{j+1/2}}{j!}. \end{aligned}$$

Then we have

$$\begin{aligned} u_1(0, k_n^2) - u_1(1, k_n^2) &\leq U_1(k_n^2) \leq u_1(0, k_n^2), \\ U_2(k_n^2) &\leq u_2(0, k_n^2), \\ U_3(k_n^2) &\leq u_3(0, k_n^2). \end{aligned}$$

Hence, based on the fact $\Gamma(1-z) = -z\Gamma(-z)$, $\Gamma(z) \approx 1/z$ as $z \rightarrow 0$, $k_n \asymp \sqrt{(q_n \log p_n)/n}/p_n \rightarrow 0$, and $a_\pi \leq \frac{\log(1-p_n^{-(1+u)})}{2\log k_n} \rightarrow 0$, it follows

$$\begin{aligned} 1 - \int_{k_n}^{k_n} g(\beta) d\beta &\leq C_1^* \left\{ u_1(0, k_n^2) - u_1(1, k_n^2) \right\} + C_2^* u_2(0, k_n^2) + C_3^* u_3(0, k_n^2) \\ &= 1 - k_n^{2a_\pi} \left\{ -\frac{\Gamma(-a_\pi)\Gamma\left(\frac{1}{2} - a_\pi\right)\Gamma(a_\pi + b)}{\sqrt{\pi}\Gamma(a_\pi)\Gamma(b)2^{a_\pi}} - C_4^* k_n^2 - C_5^* k_n^{1-2a_\pi} \right\} \\ &= 1 - k_n^{2a_\pi} \left\{ \frac{\Gamma(1 - a_\pi)\Gamma\left(\frac{1}{2} - a_\pi\right)\Gamma(a_\pi + b)}{\sqrt{\pi}\Gamma(b)2^{a_\pi}} - C_4^* k_n^2 - C_5^* k_n^{1-2a_\pi} \right\} \\ &\rightarrow 1 - k_n^{2a_\pi} \leq p_n^{-(1+u)}, \end{aligned}$$

where $C_4^*, C_5^* \geq 0$. Hence for $a_\pi \leq \frac{\log(1-p_n^{-(1+u)})}{2 \log k_n} \rightarrow 0$, we proved the first condition in (16) holds.

Now let's prove that the second condition in (16) also holds. By Theorem 1, $g(\beta) = O(|\beta|^{-2b-1})$ as $|\beta| \rightarrow \infty$. Since $\log(E_n) = O(\log p_n)$,

$$\inf_{\beta \in [-E_n, E_n]} g(\beta) = g(E_n) \approx O(E_n^{-2b-1}).$$

So

$$-\log \left(\inf_{\beta \in [-E_n, E_n]} g(\beta) \right) = (2b+1) \log(E_n) = O(\log p_n),$$

i.e., the second condition in (16) holds. Hence, all conditions in Lemma 4 are satisfied. Theorem 7 is proven. \square

B Appendix: Choosing Hyper-parameters ν and μ

Assume that q of the p variance components (λ_j) account for $(1 - \epsilon)$ proportion of the variability. That is, $\frac{\sum_{j=1}^q \lambda_j}{\sum_{j=1}^p \lambda_j} = 1 - \epsilon$, where $\lambda_{(j)}$ is the j -th largest value. Suppose that $\lambda_j \sim \text{Gamma}(\nu, \mu)$. The degree of sparsity, i.e. the number of relevant components, q can then be viewed as finding q such that the proportion achieves $1 - \epsilon$. Since the proportion is a random quantity, we seek q such that the median of the distribution of the proportion reaches equality. Note that since, μ is a scale parameter, the distribution of the proportion is unaffected by μ . Hence a grid search can be achieved to find ν such that the equation is satisfied by the median of the distribution, this just requires sampling from a Gamma $(\nu, 1)$ distribution to approximate the distribution for a given ν .

After choosing ν , we then choose the scale parameter, μ , we seek to ensure that the prior distribution for β is near zero at $p - q$ directions. To do so, recall that the distribution must lie on the ellipsoid given by $\beta^T \Sigma_X \beta = \theta \sigma^2$. Hence, we wish to push $p - q$ directions to be inside the ellipsoid, i.e. near zero. So, we set μ such that the probability of β_j under the unrestricted Normal distribution, being inside the ellipsoid is $1 - q/p$. Note that this

probability is just $P(\beta_j^2 < \theta\sigma^2)$. Now

$$\begin{aligned}
 P(\beta_j^2 < \theta\sigma^2) &= P\left(w_j < \frac{1}{\lambda_j}\right) = \int_0^\infty \int_0^{1/n\lambda_j} f_w(w_j) f_\lambda(\lambda_j) dw_j d\lambda_j \\
 &= \int_0^\infty \frac{1}{\Gamma(1/2)} \gamma\left(\frac{1}{2}, \frac{1}{2\lambda_j}\right) f_\lambda(\lambda_j) d\lambda_j \\
 &= \frac{1}{\Gamma(1/2)} E_\lambda \left[\gamma\left(\frac{1}{2}, \frac{1}{2\lambda_j}\right) \right],
 \end{aligned}$$

where w_j is a χ_1^2 random variable, and γ is the lower incomplete gamma function. This can again be evaluated on a grid. This time a grid of μ .